Rule-based and stimulus-based cues bias auditory decisions via different computational and physiological mechanisms

Nathan Tardiff[1*]

Lalitta Suriya-Arunroj[1]

Yale E. Cohen[1**]

Joshua I. Gold[2**]

[1] Department of Otorhinolaryngology, Perelman School of Medicine, University of Pennsylvania, United States

[2] Department of Neuroscience, Perelman School of Medicine, University of Pennsylvania, United States

* For correspondence: ntardiff@sas.upenn.edu

**Contributed equally

Abstract

The varied effects of expectations on auditory perception are not well understood. For example, both top-down rules and bottom-up stimulus regularities generate expectations that can bias subsequent perceptual judgments. However, it is unknown whether these different sources of bias use the same or different computational and physiological mechanisms. We examined how rule-based and stimulus-based expectations influenced human subjects' behavior and pupil-linked arousal, a marker of certain forms of expectation-based processing, during an auditory frequency-discrimination task. Rule-based cues biased choice and response times (RTs) toward the more-probable stimulus. In contrast, stimulus-based cues had a complex combination of effects, including choice and RT biases toward and away from the frequency of recently heard stimuli. These different behavioral patterns also had distinct computational signatures, including different modulations of key components of a novel form of a drift-diffusion model, and distinct physiological signatures, including substantial bias-dependent modulations of pupil size in response to rule-based but not stimulus-based cues. These results imply that different sources of expectations can modulate auditory perception via distinct mechanisms: one that uses arousal-linked, rule-based information and another that uses arousal-independent, stimulus-based information to bias the speed and accuracy of auditory perceptual decisions.

Introduction

The auditory system is sensitive to expectations (Chambers et al., 2017; Gifford, Cohen, & Stocker, 2014; Heilbron & Chait, 2018). Some expectations are instructed explicitly, such as via cues that carry information about the probability of occurrence of subsequent auditory stimuli. Other expectations are inferred explicitly or implicitly from the features of an auditory stimulus, including temporal or structural regularities. Despite the importance of both rule-based and stimulus-based expectations, we lack basic knowledge about the effects of both forms of expectations on auditory perception, including whether they use distinct or shared computational and physiological mechanisms.

One set of open questions relates to our understanding of how rule-based and stimulus-based expectations affect categorical auditory decisions. In general, for non-auditory decision tasks, rule-based expectations can lead to biases in behavioral choices and response times (RTs) that are consistent with normative principles, including a tendency to make faster and more-prevalent choices to more-probable alternatives (Dunovan, Tremel, & Wheeler, 2014; Hanks, Mazurek, Kiani, Hopp, & Shadlen, 2011; Kelly, Corbett, & O'Connell, 2020; Mulder, Wagenmakers, Ratcliff, Boekel, & Forstmann, 2012). These effects are thought to be mediated via top-down input from higher-order brain regions to earlier sensory regions (Summerfield & de Lange, 2014). However, the role of such rule-based expectations in auditory decision-making is relatively unexplored (except see de Gee et al., 2020; Gifford et al., 2014).

In contrast, stimulus-based expectations have been studied extensively and are thought to reflect, in part, bottom-up mechanisms in the auditory system, such as neural adaptation to stimulus regularities (Chambers et al., 2017; Lesicko, Angeloni, Blackwell, De Biasi, & Geffen, 2021; Nelken, 2014; Parras et al., 2017; Todorovic & de Lange, 2012; Todorovic, van Ede, Maris, &

de Lange, 2011). These adaptation-like mechanisms can have the opposite effect as rule-based cues, potentiating responses to violations of stimulus regularities and biasing perception away from recent stimuli (Alais, Orchard-Mills, & Van der Burg, 2015; Holt & Lotto, 2008; Shu, Swindale, & Cynader, 1993; Stocker & Simoncelli, 2005). However, it is also feasible that stimulus-based cues could be used to rapidly update prior beliefs, which could then bias subsequent decisions via the same top-down mechanisms used for rule-based effects (Bastos, Lundqvist, Waite, Kopell, & Miller, 2020; Bastos et al., 2012; de Lange, Heilbron, & Kok, 2018; Fischer & Whitney, 2014; Heilbron & Chait, 2018; Krishnamurthy, Nassar, Sarode, & Gold, 2017; Sotiropoulos, Seitz, & Seris, 2011; Todorovic et al., 2011; Tsunada, Cohen, & Gold, 2019).

We thus sought to answer a basic question that is fundamental to our understanding of how the brain uses rule-based and stimulus-based information to form auditory decisions: do decision biases elicited by explicit top-down rules versus those elicited by stimulus regularities use the same or different computational and physiological mechanisms? To answer this question, we recruited human subjects to perform a two-alternative, forced-choice frequency-discrimination task. These subjects reported whether a test stimulus (a tone burst that was embedded in a noisy background) was “low frequency” or “high frequency.” We manipulated both the signal-to-noise ratio (SNR) of the test stimulus (relative to the background) and two types of expectation-generating cues: 1) rule-based cues, in the form of visual stimuli indicating the probability of each test stimulus; and 2) stimulus-based cues, in the form of temporal sequences of tone bursts, akin to those used to study stimulus-specific adaptation and mismatch negativity (Näätänen, Paavilainen, Rinne, & Alho, 2007; Nelken, 2014; Sussman, 2007), that immediately preceded presentation of the test stimulus. We also measured the subjects’ pupil diameter, which is a

physiological marker of arousal that is sensitive to certain cognitive processes related to decision-making (Joshi & Gold, 2020), including decision biases (de Gee et al., 2017; de Gee, Knapen, & Donner, 2014; de Gee et al., 2020; Krishnamurthy et al., 2017; Urai, Braun, & Donner, 2017) and violations of top-down, but not bottom-up, expectations (Filipowicz, Glaze, Kable, & Gold, 2020). We found that rule-based and stimulus-based behavioral biases exhibited distinct computational and physiological (i.e., pupillometric) signatures that may reflect differential contributions of top-down and bottom-up forms of expectation-dependent information processing in auditory perceptual decision-making.

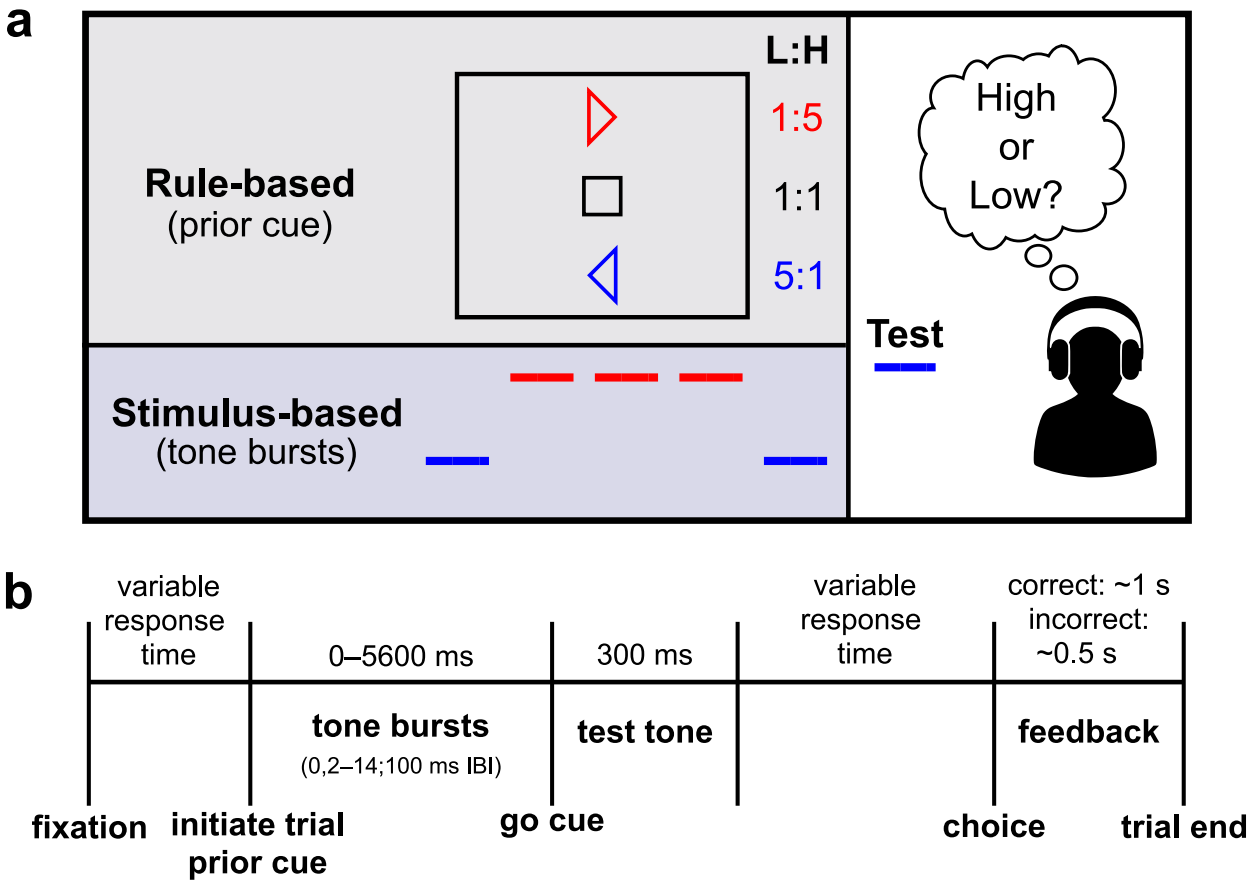

Figure 1. Task structure. **a** Subjects indicated with a button press whether a test tone was "high frequency" or "low frequency." In the rule-based condition, the test tone was preceded by a visual stimulus (prior cue) that indicated the probability that the upcoming tone would be low (L) or high (H) frequency, with the probability determined by the L:H ratio. In the stimulus-based condition, the test tone was preceded by a variable-length, temporal "pre-test" sequence of low- and high-frequency tone bursts. On average, this sequence was not predictive of the test tone. In the mixed conditions, subjects received both rule-based and stimulus-based cues on each trial. **b** Detailed trial timing. After attaining fixation, the subject initiated the trial with a button press. The subject was then able to report their decision with a second button press at any time following the "go cue" (up to 2000–3000 ms).

Results

Fifty human subjects performed a frequency-discrimination task in which they indicated with a button press whether a test stimulus was high frequency or low frequency (Figure 1). Task difficulty was titrated by embedding the test stimulus in a background of white noise of various signal-to-noise ratios (SNRs). We manipulated prior information in a blockwise fashion for each subject. In the rule-based condition, prior to stimulus onset (Figure 1), one of three visual cues indicated the probability that the upcoming test stimulus would be low frequency or high frequency (high:low ratio = 1:5 (low), 1:1 (neutral), or 5:1 (high)). In the stimulus-based condition, prior information was manipulated by presenting a temporal sequence of tone bursts (using the maximum SNR; 2–14 bursts per trial) prior to the test stimulus. This "pre-test" sequence varied in terms of its pattern of low and high frequencies but, on average, was not predictive of the frequency of the test tone. We also presented mixed conditions in which subjects encountered both rule-based and stimulus-based cues on each trial.

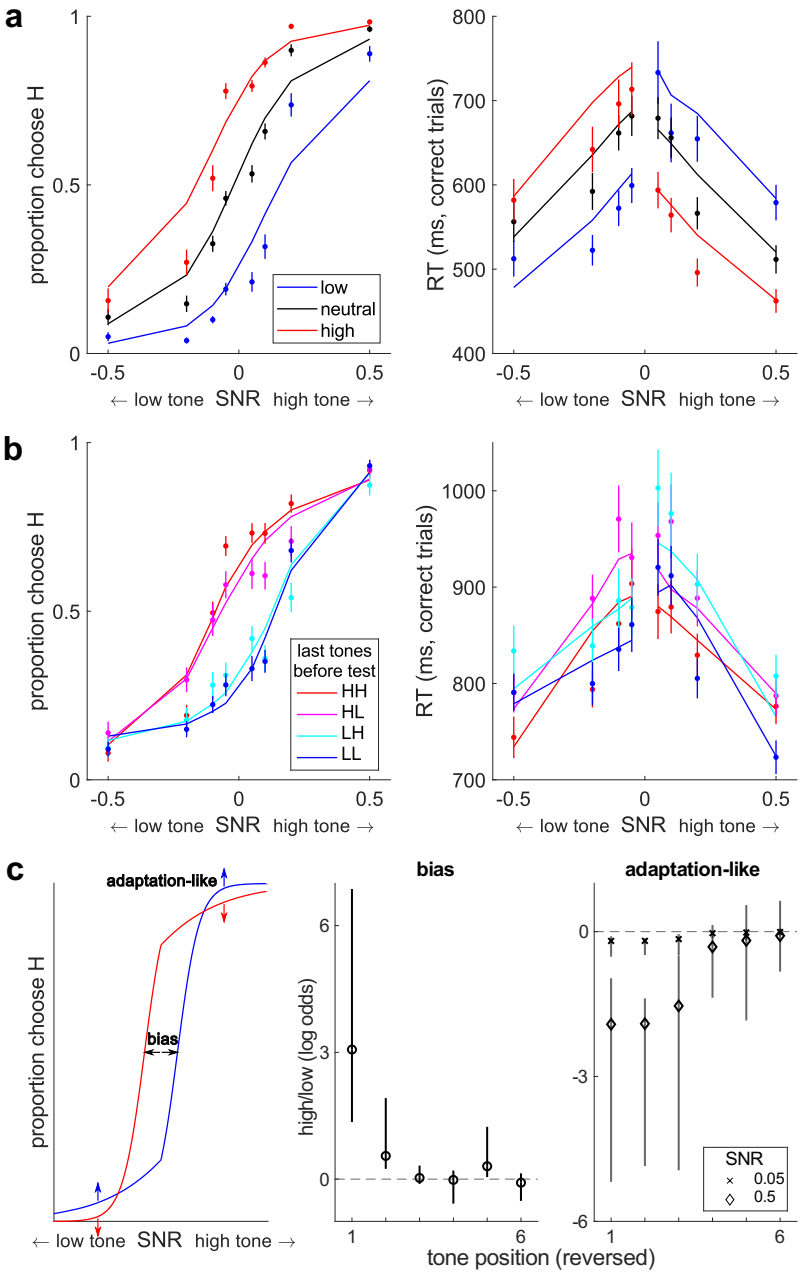

Figure 2. Behavioral summary. **a** Psychometric (left) and chronometric (right) functions from the rule-based condition for each prior cue (see legend). **b** Psychometric (left) and chronometric (right) functions from the stimulus-based condition for different patterns of the last two pre-test tone bursts (see legend; HH = the last two tones were high, HL = the last tone was high and the second-to-last tone was low, etc.). In **a** and **b**, data points are averages over all subjects, and error bars are standard errors of the mean (SEM). Solid lines are DDM fits (see text). By convention, positive and negative SNRs are low-frequency and high-frequency test tones, respectively. **c**

Left: Schematic illustrating how choice effects in the stimulus-based condition can be decomposed into: 1) a bias that shifts the psychometric function in favor of the most-recently heard tones, which dominates at low absolute SNRs; and 2) an adaptation-like effect that decreases sensitivity to the most-recently heard tones, which becomes prominent at high absolute SNRs. Blue and red curves illustrate simulated psychometric functions corresponding to trials in which the last pre-test tone burst was low or high frequency, respectively. Right: Logistic analysis of the bias and adaptation-like effects in the stimulus-based condition, as a function of pre-test tone-burst position (1 = the tone just prior to the test tone, etc.). Values along the ordinate are the median effect of a pre-test tone at that position on choice, measured as log-odds ratios for high/low frequency (positive/negative values imply that a high-frequency tone at the given position increases/decreases the odds of choosing high-frequency relative to low-frequency tones). Error bars are bootstrapped 95% confidence intervals (10,000 samples).

Rule- and stimulus-based biases had different effects on choices and RTs

In the rule-based condition, the subjects' choices and RTs showed consistent biases in accordance with the prior cues (Figure 2a). In particular, the subjects tended to choose the more-probable option more often and more quickly than a neutral or less-probable option. For example, when the prior cue indicated that the test tone was more likely to be high frequency, subjects chose high frequency more often and responded faster. To quantify these effects, we fit logistic and linear models to the subjects' choices and mean RTs from correct trials, respectively. The choice bias was well-characterized as an additive shift (bias) of the psychometric function in favor of the prior (mean ΔAIC no bias versus bias = 54.60). These fits were only marginally improved by allowing the slope (sensitivity) of the psychometric function to vary with the prior (mean ΔAIC bias vs. bias + sensitivity = 0.29). A Bayesian random-effects analysis confirmed the bias-only model as the most likely model (protected exceedance probability = 0.82).

The RTs included a sharp discontinuity within the low- and high-prior conditions depending on whether subjects chose with ("congruent"; i.e., the prior and choice were toward the same frequency) or against ("incongruent"; i.e., the prior and choice were toward opposite frequencies) the cued prior (modulation by congruence, $F(2,65.08) = 160.43$, $p < 0.0001$). For example, on average, RTs at the lowest SNR were >100-ms faster when subjects chose high frequency with a high-prior cue or low frequency with a low-prior cue than when they made a choice incongruent with the prior (Figure 2a, right). Congruent RTs were faster than both incongruent RTs ($B = 128.17$, $t(226.27) = 17.83$ $p_{\text{corrected}} < 0.0001$) and RTs on neutral prior trials ($B = 75.48$, $t(51.03) = 9.19$, $p_{\text{corrected}} < 0.0001$), whereas incongruent RTs were slower than neutral-prior RTs ($B = -52.69$, $t(49.30) = -6.04$, $p_{\text{corrected}} < 0.0001$). Thus, the prior cues resulted in choices that, on average, were more common and faster to the more probable alternative.

In the stimulus-based condition, the subjects' choices and RTs showed a more complex pattern. Figure 2b shows choices and RTs plotted as a function of the last two pre-test tone bursts for a given trial. At low SNRs of the test stimulus, choices were biased toward the frequency of the most-recently heard tones, and RTs were faster when the choice was congruent with the most-recently heard tone. These effects are evident in the lateral shifts in the psychometric function and discontinuities (vertical shifts) in the RTs at low SNRs and are consistent with the rule-based effects (see Figure 2a). In contrast, at higher test SNRs, an adaptation-like effect was more prominent, such that subjects were, on average, more likely and faster to respond with the alternative that was incongruent with the most-recently heard tones. For example, subjects were more likely and faster to respond "high frequency" after having heard two low-frequency tones than after having heard two high-frequency tones (Figure 2b, blue data points vs. red data points at SNR = 0.5; see also Figure 2c, left).

To decompose these different effects of the pre-test tone sequence on choice and estimate the contributions of individual tone bursts, we fit a logistic model that included for each tone-burst position: 1) an additive bias term describing the degree to which choice was biased in the same (positive values) or opposite (negative values) direction as the frequency of that tone burst; and 2) an SNR-dependent, adaptation-like term describing the change in discriminability attributable to that tone burst, in which negative values corresponded to incongruent choices. These fits yielded, on average, a positive bias and a negative SNR-dependent adaptation-like component. Both the bias and adaptation-like terms had a strong recency effect in which the final 2–3 tone bursts just before the test tone made the strongest contributions to choice (Figure 2c, right). This bias + adaptation model was favored over both a bias-only model (mean ΔAIC = 2.22) and a model that did not include an effect of the tone bursts (mean ΔAIC = 56.85). A Bayesian

random-effects analysis confirmed the bias + adaptation model as the most likely (protected exceedance probability = 0.86). This negative adaptation effect was unique to the stimulus-based condition: adaptation-like terms estimated in the rule-based condition did not differ significantly from 0 (sign test, all ps > 0.05).

For the stimulus-based condition, we found similarly complex effects for average correct RTs across subjects, which showed a main effect of congruence ($F(3,74.02) = 27.76$, $p < 0.0001$) and an SNR×congruence interaction ($F(3,197.17) = 11.58$, $p < 0.0001$). This interaction included a tendency for faster/slower RTs when the last two pre-test tone bursts were congruent versus incongruent with choice at the lowest/highest SNR (post-hoc test of interaction, $B = 112.26$, $t(442.16) = 5.06$, $p_{\text{corrected}} < 0.0001$). In summary, the subjects' choices were biased to be congruent with the most-recently heard pre-test tone bursts at low SNRs but were biased to be incongruent with those tone bursts at high SNRs. Together, these findings suggest the possibility of separate computational mechanisms for the rule-based and stimulus-based effects, which we examine next in more detail.

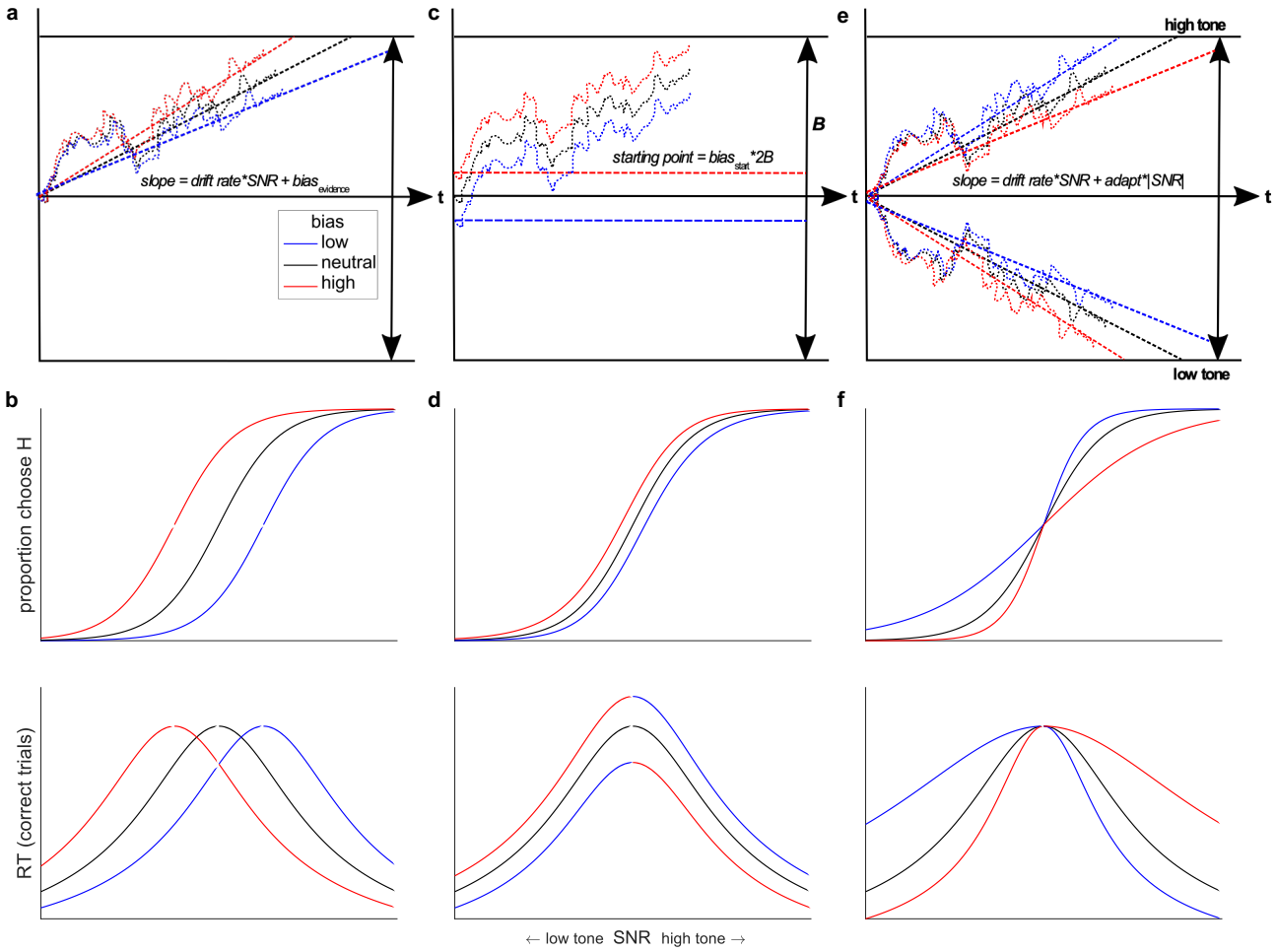

Figure 3. Simulated DDM bias terms (top) and their predicted, distinguishable effects on psychometric (choice; middle) and chronometric (RT; bottom) functions. **a** A bias implemented as an additive offset to the drift-rate term, which shifts the slope of the decision variable in the direction favored by the bias. **b** This evidence-accumulation bias causes lateral shifts in the psychometric and chronometric functions, corresponding to more and faster choices in the direction of the bias. **c** A bias implemented as a shift in the starting point of evidence accumulation toward the bound favored by the bias, implying that less evidence is needed to make a bias-congruent choice. **d** This starting-point bias causes smaller lateral shifts in the psychometric function than for the evidence-accumulation bias and vertical asymmetries in the chronometric function (see the discontinuity at SNR = 0) such that RTs are faster (slower) for prior congruent (incongruent) choices. **e** An adaptation-like bias that affects the slope of the decision variable in a manner that varies with the absolute value of the test-tone SNR. **f** For the stimulus-based condition, this term, which is absent at SNR = 0 and increases with increasing

|SNR| of the test tone, shifts the slope of the decision variable away from the frequency of the tone bursts heard prior to the test tone and thus causes more and faster choices to the frequency opposite the most-recently heard pre-test tone bursts. **a,c,e** Dotted lines: example evolutions of the decision variable for a single trial with a given bias (see legend). Dashed lines: average slope of decision variable. t = time. In **c**, *B* = total bound height/2. **b,d,f** Simulated choice (top) and RT (bottom) data from an analytical solution to the DDM (Palmer, Huk, & Shadlen, 2005).

Rule- and stimulus-based biases were captured quantitatively by drift-diffusion model fits

To better identify the computations responsible for these effects, we fit DDMs to the behavioral data from each task condition (Shinn, Lam, & Murray, 2020). Unlike the regression-based approaches above, DDMs can jointly account for choice and RT data in a unified framework. In the DDM, noisy evidence is accumulated to a pre-defined bound, which we modeled using five free parameters: 1) *drift rate,* which influences the rate at which the test stimulus contributed to evidence accumulation; 2) *bound height,* or the total evidence required to commit to a decision at the beginning of the trial; 3) *bound slope*, which determined the rate of a linear "collapse" of the bound over the course of a trial (i.e., a bound that decreases in height over time), to account for potential urgency effects resulting from the time pressure to make the decision before the trial was aborted after 2–3 s; 4) *non-decision time,* or the portion of total reaction time that was not determined by decision formation (e.g., sensorimotor processing); and 5) *lapse rate*, or error rates for easily perceivable stimuli.

We added several terms to each model to account for bias effects (Figure 3). For the rule-based condition, we used two additional free parameters per prior cue to account for biases in: 1) the rate of accumulation, and 2) the starting point of the evidence-accumulation process. For the stimulus-based condition, we used three additional parameters: 1) a bias in the rate of evidence accumulation, 2) a bias in the starting point of the evidence-accumulation process, and 3) a shared time constant that describes the rapid temporal decay in the influence of each pre-test tone burst on the two biasing parameters (i.e., an exponentially weighted sum of biasing effects caused by each preceding burst; Figure 2c, right). Positive/negative values for these bias terms corresponded to more and faster choices toward/away from the dominant frequency of the pre-test tone burst sequence (i.e., of the exponentially weighted sum).

We introduced an additional mechanism to account for adaptation-like effects in the stimulus-based condition by modulating the strength of evidence in an SNR-dependent fashion (Figure 3c, d). Given the sharp decline in the effect of individual tone bursts (Figure 2c, right) and previous work suggesting an exponential decay of auditory neural adaptation (Nelken, 2014; Pérez-González, Hernández, Covey, & Malmierca, 2012), we again modeled the adaptation-like effect of the tone bursts as an exponentially weighted sum of the effects from each preceding tone burst (with a shared time constant but separate, multiplicative weights for high- and low-frequency tone bursts), which was then multiplied by the SNR of the test tone. Positive/negative weights imply that repeated pre-test tone bursts caused more and faster choices toward/away from the repeated tone frequency. Finally, we introduced an additional parameter to increase non-decision time as a function of the absolute value of the stimulus-based bias, to capture the tendency for faster RTs when the last two pre-test tone bursts were the same frequency (post-hoc test of interaction, $B = 68.83$, $t(72.07) = 7.76$, $p < 0.0001$).

These models captured the patterns of bias and adaptation-like effects in the choice and RT data (Figure 2a, b; solid lines). In the rule-based condition, the full model with cue-dependent bias terms provided a better fit to the data than either the "collapsing-bound model" without cue-dependent biases or a "base model" with neither cue-dependent biases nor a collapsing bound (Table 1; protected exceedance probability = 1). Similarly, in the stimulus-based condition, a model with tone-burst-dependent biases outperformed models without these biases, and the full model with both bias and SNR-dependent terms provided the strongest fit to the data (Table 1; protected exceedance probability = 1). Furthermore, the SNR-dependent terms were consistently negative, confirming an adaptation-like effect (one-sample t-test; both $p\text{s}_{\text{corrected}} < 0.0001$).

condition	model	number of parameters	mean AIC	protected exceedance probability
rule-based				
	base	6	–66.00	0
	collapsing bound	7	–149.82	0
	full	11	–267.28	1
stimulus-based				
	base	6	211.52	0
	collapsing bound	7	133.29	0
	collapsing bound + stimulus-based bias	11	76.85	0
	full	14	52.02	1

Table 1. DDM model-fit comparisons. In both conditions, the full model was favored over reduced models, with the lowest AIC and a protected exceedance probability = 1. All models included evidence-acculumulation and starting-point bias terms to account for idiosyncratic biases, even when they did not include cue-dependent biases. See Methods for full implementation details.

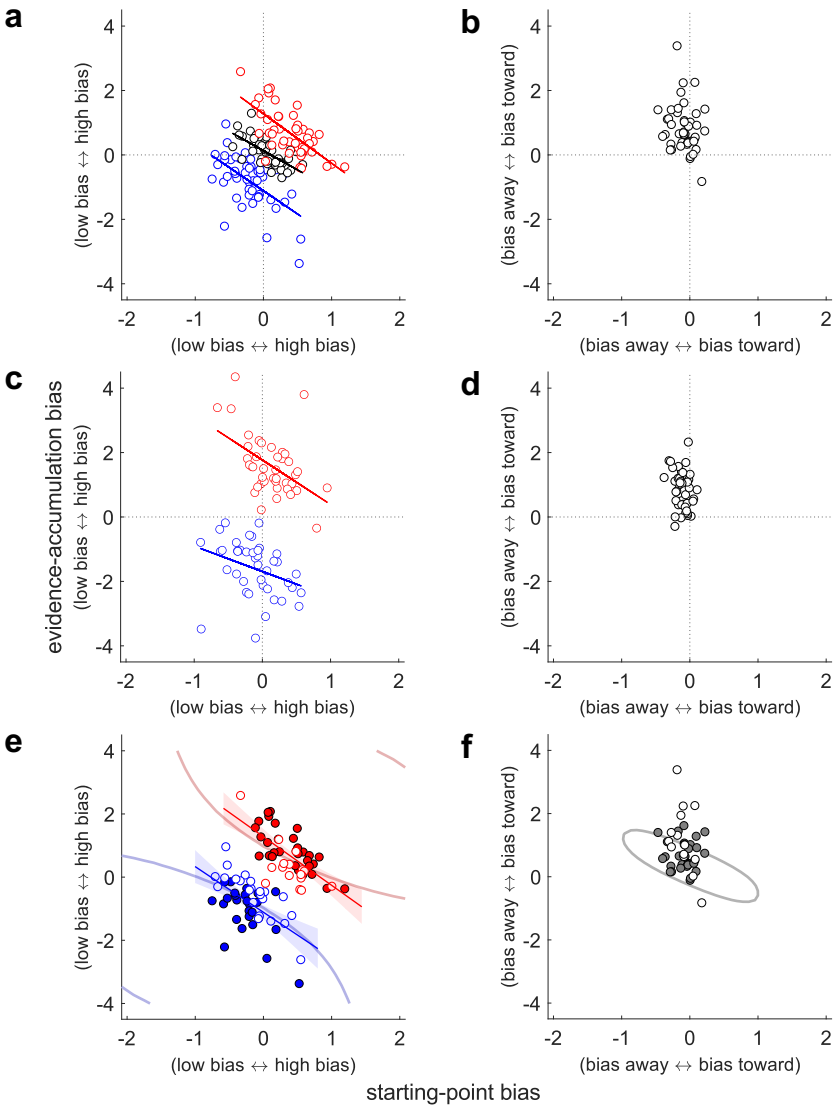

Figure 4. Different computational signatures of rule- and stimulus-based biases. Each panel shows best-fitting evidence-accumulation (ordinate) and starting-point biases, plotted per subject (points). **a** Data from the rule-based condition, for each of the three prior cues (blue: low, black: neutral; red: high). Lines are linear fits ($p < 0.05$). **b** Data from in the stimulus-based condition (no linear relationship). **c** Data from the rule-based mixed condition, plotted as in **a**. **d** Data from the stimulus-based condition, plotted as in **b** (no linear relationship). **c** and **d** show results for the mixed-condition 1, which included block-level prior cues; results were similar in mixed-condition 2, which had trial-wise priors. **e** Data from **a** (the low- and high-prior conditions) plotted with respect to optimal performance contours from the rule-based condition. The average 97% contours (curved lines) demarcate the area of the parameter space in which choice accuracy

is at least 97% of the maximum possible accuracy. Accuracy was predicted by the DDM applied to the actual task sequences. Closed/open circles indicate that the data fell within/outside of the subject-specific 97% contour. Lines are linear fits as in **a**, and shaded regions are 95% confidence intervals. **f** Same as **e**, but for the stimulus-based condition. The 97% contour is for the context of two low-tone bursts before the test tone (similar results were obtained for two high-tone bursts but not shown).

Rule- and stimulus-based biases exhibited distinct computational signatures

The rule- and stimulus-based bias effects had distinct computational signatures. For the rule-based condition, subjects tended to use both starting-point and evidence-accumulation biases in the direction of the higher-probability alternative (Table 2, light green rows; one sample *t*-test, all $ps_{\text{corrected}} < 0.0001$). Across subjects, these two kinds of computational biases were negatively correlated with one another: subjects who tended to use stronger starting-point biases had weaker evidence-accumulation biases and vice versa. This negative relationship was evident within all three prior cue conditions (Figure 4a; low: Spearman's $\rho = -0.49$, $p_{\text{corrected}} = 0.0003$; neutral: $\rho = -0.72$, $p_{\text{corrected}} < 0.0001$; high: $\rho = -0.62$, $p_{\text{corrected}} < 0.0001$).

condition	rule-based		stimulus-based		mixed 1		mixed 2		
parameter	**mean**	**SD**	**mean**	**SD**	**mean**	**SD**	**mean**	**SD**	**description**
v_{SNR}	6.51	3.36	4.97	2.55	4.40	2.34	5.46	3.21	drift rate
B	0.92	0.26	1.02	0.27	1.06	0.21	0.93	0.17	bound height (total bound height = 2B)
t_B	0.92	0.48	0.80	0.33	1.01	0.38	0.87	0.45	bound slope
ndt_0	0.27	0.08	0.46	0.07	0.38	0.05	0.07	0.07	non-decision time (s)
ndt_{Bias}	*	*	−0.12	0.29	−0.12	0.32	−0.17	0.29	modulation of non-decision time by absolute stimulus-based bias
λ	0.02	0.01	0.02	0.02	0.02	0.01	0.02	0.01	lapse rate
v_{Low}	−0.83	0.79	*	*	−1.60	0.85	−1.36	0.91	Evience-accumulation bias for low prior
v_0	0.07	0.41	−0.20	0.62	*	*	−0.19	0.61	Evidence-accumulation bias for neutral prior (idiosyncratic)
v_{High}	0.67	0.71	*	*	1.59	0.93	1.19	1.04	Evidence-accumulation bias for high prior
v_{Bias}	*	*	0.84	0.73	0.83	0.60	0.80	0.49	stimulus-based evidence-accumulation bias
τ_{Bias}^{-1}	*	*	4.99	4.89	6.82	5.24	7.80	5.11	time constant of stimulus-based bias
va_{Low}	*	*	−2.31	1.81	−2.05	1.83	−1.97	1.37	adaptation weight, low tones
va_{High}	*	*	−1.40	1.75	−1.53	1.67	−1.68	1.22	adaptation weight, high tones
τ_{va}^{-1}	*	*	7.04	6.25	9.84	5.45	8.74	5.97	time constant of adaptation
z_{Low}	−0.20	0.31	*	*	−0.12	0.36	0.00	0.30	starting point bias for low prior
z_0	0.06	0.22	−0.03	0.19	*	*	0.02	0.24	starting point bias for neutral prior (idiosyncratic)
z_{High}	0.39	0.31	*	*	0.13	0.33	0.03	0.35	starting point bias for high prior
z_{Bias}	*	*	−0.09	0.16	−0.11	0.10	−0.03	0.17	stimulus-based starting-point bias

Table 2. Mean and standard deviation (SD) of best-fitting paramaters across subjects. Green rows: rule-based bias parameters; yellow rows: stimulus-based bias parameters; * parameter not present in that condition. See Methods for a fuller description of the parameters.

For the stimulus-based condition, subjects also tended to use a combination of starting-point and evidence-accumulation biases but with a different pattern than for the rule-based condition (Table 2, light yellow rows). Specifically, the evidence-accumulation bias tended to be positive (i.e., toward the frequency of the most recent tone bursts; one-sample *t*-test, $p < 0.0001$). In contrast, the starting-point bias tended to be in the opposite direction, away from the bound for the frequency of the most recent tone bursts ($p = 0.0007$). Unlike for the rule-based DDM fits, we could not identify any correlation between best-fitting values of evidence-accumulation and starting-point biases across subjects (Figure 4b; Spearman's $\rho = -0.20$, $p = 0.19$). In the mixed-condition trials, we confirmed that this differential pattern of correlations was also present and thus was not simply an idiosyncratic quirk of either the rule- or stimulus-based condition tested individually (rule-based: Figure 4c, all $p\text{s}_{\text{corrected}} < 0.005$; stimulus-based: Figure 4d, all $p\text{s} > 0.05$).

The negative relationship between evidence-accumulation and starting-point biases in the rule-based conditions is similar to that found for monkeys performing a reward-biased visual-decision task (Doi, Fan, Gold, & Ding, 2020; Fan, Gold, & Ding, 2018). That reward-driven relationship was interpreted in terms of coupled, goal-directed (top-down) adjustments to the decision process that improved performance. Specifically, monkeys made adjustments in evidence-accumulation and starting-point biases that were sensitive to session- and monkey-specific variations in perceptual sensitivity and contextual factors. These adjustments maintained near-optimal or "good enough" (satisficing) performance, possibly by using a gradient-ascent-like learning process to rapidly adjust the biases until reaching a performance plateau. Critically, the contours of this performance plateau showed a "tilt" in the space of evidence-accumulation and starting-point biases, such that negatively correlated values of these biases traced out iso-

performance contours. We reasoned that a similar sensitivity to performance-satisficing combinations of biases could plausibly underlie the correlation between the evidence-accumulation and starting-point biases in our rule-based condition.

To assess this possibility, we used the DDM to predict, for each subject, the average choice accuracy that could be achieved across a range of evidence-accumulation and starting-point bias parameters, given the subject's other fit parameters and the task context. For the rule-based condition, task context was determined by the prior cue. For the stimulus-based condition, task context was defined with respect to two high or two low pre-test tone bursts, which had the strongest effects on behavior in that condition. To facilitate comparisons, we normalized predicted accuracy for each subject and condition to the maximum value achieved via simulations using a wide range of evidence-accumulation and starting-point bias parameter values.

For the rule-based condition, the subjects' combinations of evidence-accumulation and starting-point biases tended to yield nearly optimal performance (low: median proportion maximum performance = 0.97, range = [0.76–1.00]; neutral: 1.00 [0.97–1.00]; high: 0.98 [0.86–1.00]). Furthermore, the location and tilt of the across-subjects distribution of biases appeared qualitatively to respect the tilt of the plateau of the performance function (Figure 4d), suggesting that sensitivity to this plateau was a potential cause of the correlation between the biases. For the stimulus-based condition, the subjects' biases also yielded nearly optimal performance (LL: median proportion max performance = 0.99, range = [0.62–1.00]; HH: 0.99 [0.80–1.00]), reflecting the fact that some degree of positive bias was needed to offset performance decrements induced by the adaptation-like effect. However, the subjects' biases for the stimulus-based condition did not follow the tilt of the plateau of the performance function (Figure 4e).

To confirm this pattern of results, we used a mixed-effects model to compare the slopes of the linear fit that predicted the starting-point bias from the evidence-accumulation bias between the different contexts. We could not identify any difference in the slopes of the high versus low biases within the rule-based condition ($B = -0.03$, $t(126.00) = -0.14$, $p > 0.05$). In contrast, there was a significant difference in the slope of the biases between the rule-based and stimulus-based conditions ($B = 0.45$, $t(126.00) = 2.80$, $p = 0.006$). Together, these findings are consistent with the idea that the participant's choices in the stimulus-based condition were produced by a different underlying mechanism than the coupled (tilted) changes that mediated choices in the rule-based condition.

Consistent with this idea of different mechanisms, we could not find any evidence that individual subjects made consistent use of starting-point and/or evidence-accumulation biases across the rule-based and stimulus-based conditions. Specifically, there was no correlation between best-fitting values of each bias term computed per subject when comparing across the two conditions (ps > 0.05 for both starting-point and evidence-accumulation biases). When rule-based and stimulus-based biases were used at the same time in the mixed conditions, we also could not identify a correlation between the bias terms (all $ps > 0.05$; note that parameter ranges were similar for the single and mixed blocks, suggesting that the subjects used the biases in a roughly comparable, although not identical, way in the two block types; Table 2). Together, these results suggest that rule-based and stimulus-based biases rely on separable computational processes, potentially reflecting differences in top-down and bottom-up sources of expectations.

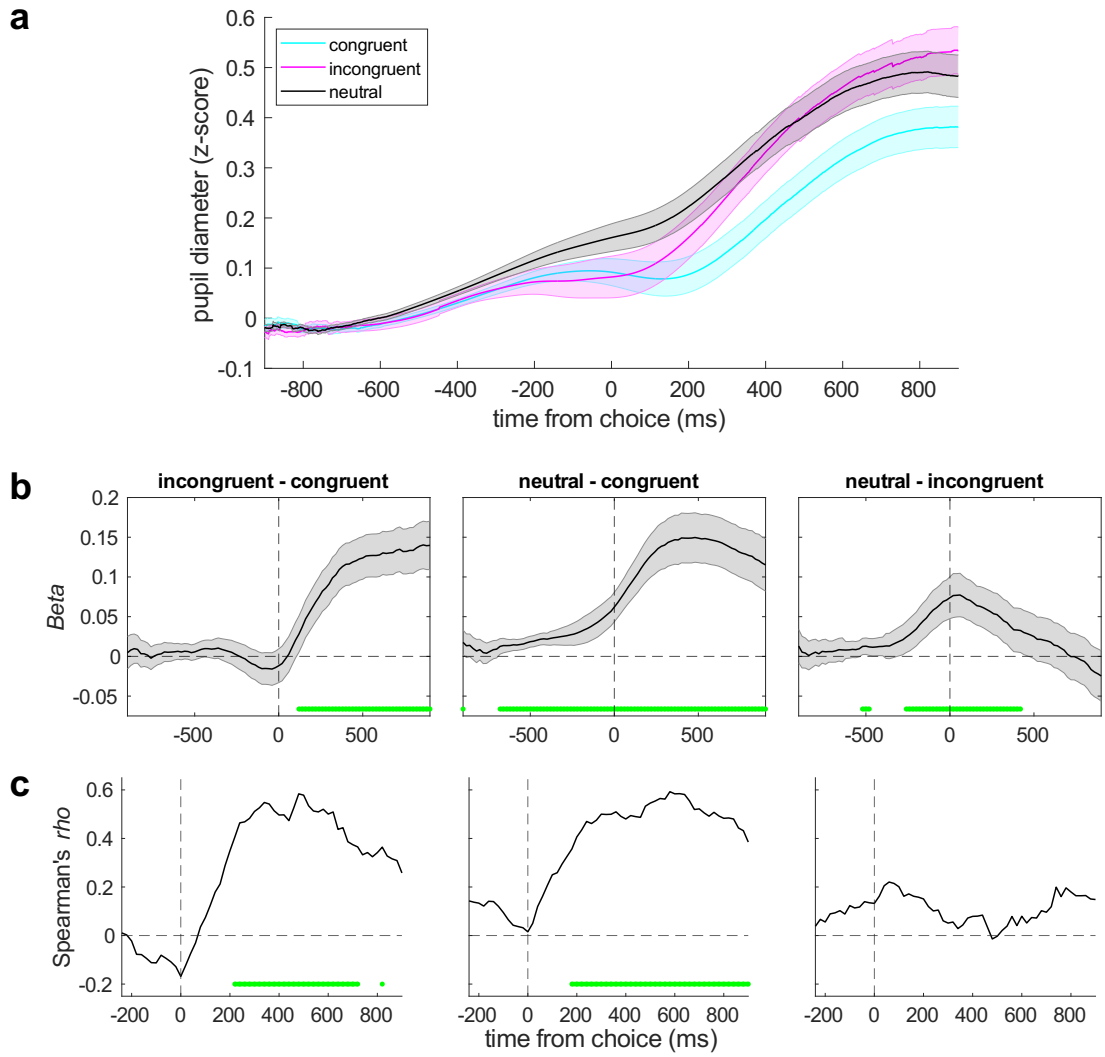

Figure 5. **Rule-based cues strongly modulated pupil-linked arousal**. **a** Pupil diameter on correct trials, aligned to choice and plotted as a function of the congruence between the choice and the prior. Lines and error bars are means and SEM across all trials and subjects. **b** Regression coefficients (beta values) from a linear mixed-effects model as a function of different pupil contrasts (see labels above each panel). Error bars are 95% confidence intervals of the parameter estimates. **c** Across-subject Spearman correlation between: 1) the degree to which each subject was biased by the prior cues, estimated from a logistic regression model of choice behavior; and 2) each subject's pupil contrast from a linear regression model. Values in **b** and **c** were computed in 20 ms-wide time bins. Green lines indicate time bins for which $p_{\text{corrected}} < 0.05$, FDR-corrected across time and contrast. Figure 5 – Supplement 1 presents the same analyses as in **a** and **b** for incorrect trials.

Rule- and stimulus-based biases exhibited distinct physiological signatures

Because pupil dilation is associated with behavioral decision biases (de Gee et al., 2017, 2014, 2020; Krishnamurthy et al., 2017; Urai et al., 2017), we tested whether and how pupil size was modulated by our rule-based and stimulus-based task conditions. In particular, we tested whether these modulations could help distinguish different forms of biases across individuals and task conditions. If pupil-linked arousal facilitates overcoming biases, then we would expect larger evoked pupil responses when comparing incongruent to congruent trials: responding correctly on incongruent trials requires overcoming bias. Furthermore, if the rule- and stimulus-based biases depend on overlapping neurophysiological mechanisms, then we would expect similar profiles of pupil responses for both conditions. In contrast, if pupil-linked arousal for our task is more sensitive to top-down than to bottom-up influences, as has been reported for other tasks (Filipowicz et al., 2020), then we would expect more strongly modulated pupil responses in the rule-based than in the stimulus-based condition.

In the rule-based condition, the choice-locked evoked pupil response was modulated strongly by congruence (Figure 5**a, b**). Specifically, the pupil response was larger for incongruent relative to congruent choices, an effect that emerged shortly after choice (because the effects were similar but weaker when aligned to stimulus versus choice onset, the figures and analyses focus on choice-aligned effects). We found a similar effect on incorrect trials (Figure 5 – Supplement 1), which implies that these pupil modulations were more closely related to the congruency between the prior and the choice than to the congruency between the prior and the stimulus. Pupil diameter was also modulated on both congruent and incongruent trials relative to neutral trials, with larger dilations on neutral trials starting before stimulus onset that likely reflected higher uncertainty on those trials (i.e., a less-informative prior; Figure 5**a**,**b**). In the mixed condition,

similar rule-based modulations were also evident and thus were robust to the presence or absence of stimulus-based biases (mixed-effects models comparing average pupil responses 220–720 ms post-choice for pairs of prior cues, all $p\text{s}_{\text{corrected}} < 0.03$, except for the no prior – incongruent contrast in mixed block 2, $p > 0.05$).

The magnitude of these rule-based pupil modulations was correlated with the magnitude of behavioral biases across subjects. Specifically, we measured the Spearman correlation coefficient between the magnitude of choice bias derived from the logistic fits to each subject's choice data (high-frequency cue bias minus low-frequency cue bias) and pupil contrast (β value). We found positive correlations ~200–800 ms post-choice for both the congruent–incongruent and neutral–congruent contrasts. In other words, a greater reliance on the prior cues corresponded to more differentiated arousal responses between trials when the cue was or was not congruent with the choice. These results complement earlier findings that pupil responses can reflect the magnitude of (inappropriate) choice biases, with larger pupil responses typically corresponding to a reduction in bias (de Gee et al., 2017, 2014, 2020; Krishnamurthy et al., 2017). Taken together with our results, these findings suggest that our subjects, particularly those who were highly sensitive to the prior cues, needed to mobilize additional resources to overcome the prior or make decisions in the absence of an informative prior.

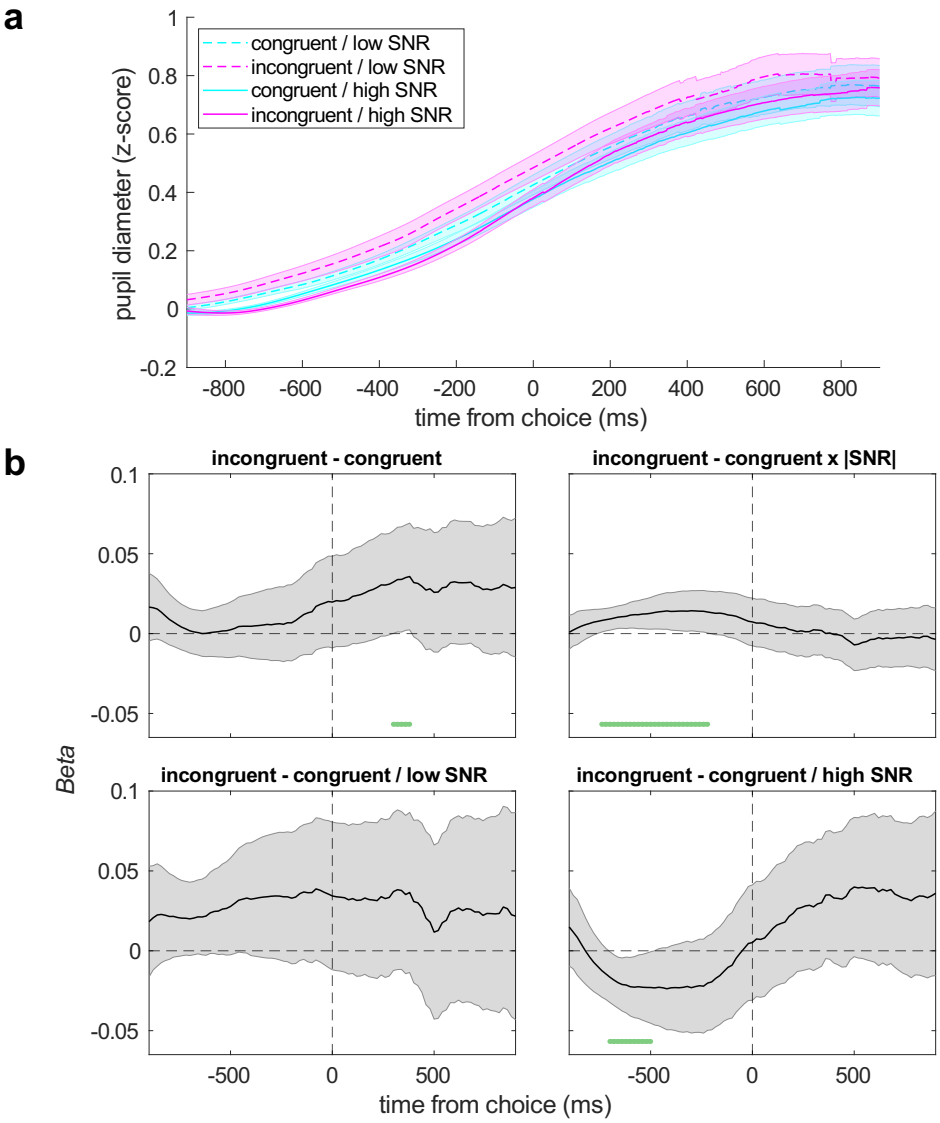

Figure 6. Stimulus-based cues weakly modulated pupil-linked arousal. **a** Pupil diameter on correct trials, aligned to choice and plotted as a function of the congruence of the choice and the most-recently heard pre-test tone bursts, separated by SNR. We only used pre-test sequences ending in two of the same tone (i.e., LL, HH) and at the lowest or highest test SNR for this analysis. Lines and error bars are means and SEM across all trials and subjects. **b** Regression coefficients (beta values) from a linear mixed-effects model for different pupil contrasts. Error bars are 95% confidence intervals of the parameter estimates. Values were computed in 20 ms-wide time bins. Dark green lines indicate time bins for which $p_{\text{uncorrected}} < 0.05$.

429 In contrast, evoked pupil diameter in the stimulus-based condition displayed a very different
430 pattern of results. Because the subjects' behavior in this condition was dependent on congruence
431 and SNR, we analyzed pupil diameter as a function of the interaction between: 1) the congruence
432 of choice with the last two pre-test tone bursts, and 2) SNR. We focused on trials in which both
433 tone bursts were the same and for only the lowest or highest test SNR values, to increase our
434 chances of finding effects. However, unlike for the rule-based condition, we did not identify any
435 effects that survived correction for multiple comparisons (Figure 6). Further, we found a
436 significant congruence×condition interaction (mixed-effects model comparing average pupil
437 responses 0–1000 ms post-choice, $B = 0.09$, $t(38.36) = 5.65$, $p < 0.0001$), which confirmed that
438 the arousal response was stronger in the rule-based condition than in the stimulus-based
439 condition. Although we could not identify any sign of stimulus-based effect in the post-choice
440 period, we found a congruence×SNR interaction at an uncorrected $p < 0.05$ from 740–220 ms
441 before choice. We also reanalyzed the rule-based condition to look for a similar
442 congruence×SNR interaction and could not identify any effect (all ps > 0.05).

443 In summary, pupil-linked arousal strongly differentiated between the rule- and stimulus-based
444 biases in the locus, strength, and timing of the effect. In the rule-based condition, pupil diameter
445 following choice was robustly indicative of the congruence of the choice and the prior cue in a
446 manner that reflected individual behavioral biases. In the stimulus-based condition, pupil
447 diameter preceding choice only weakly reflected the SNR-dependent choice congruence effects.

448

Discussion

This work was motivated by the realization that, despite an abundance of studies on the importance of expectations in auditory processing, we lack a basic understanding of their effects on perception. We focused on how human auditory perceptual decisions are influenced by two different sources of expectations, one from instructed rules that indicated the probability of the upcoming test tone and the other from stimulus regularities akin to those used in oddball tasks. Rule-based cues consistently biased behavioral choices and RTs in favor of the more probable alternative. In contrast, stimulus-based cues elicited different biases that depended on the test-tone SNR. We leveraged model fits and measures of pupil-linked arousal to show that the rule-based and stimulus-based behavioral biases have distinct computational and physiological signatures: we found coordinated computational adjustments and strong pupil modulations in the rule-based condition but not in the stimulus-based condition.

Our results extend previous findings in three fundamental ways. First, we decomposed the effects of stimulus regularities on auditory perception into an adaptation-like effect on stimulus sensitivity and a decision bias. This decomposition allowed us to directly compare decision biases produced by rule-based versus stimulus-based cues. Second, we found that rule-based and stimulus-based biases have distinct computational signatures. In particular, the effects on the decision variable (i.e., evidence-accumulation bias in the DDM) and the decision rule (i.e., starting-point bias in the DDM) are coupled for rule-based biases but not for stimulus-based biases. Third, we showed that rule-based and stimulus-based biases also have distinct physiological signatures: pupil-linked arousal is modulated by rule-based biases but not by stimulus-based biases. As detailed below, we interpret these results in terms of two potentially distinct mechanisms for incorporating prior expectations into auditory perceptual decisions, one

using top-down processing for rule-based cues and the other using bottom-up processing for stimulus-based cues.

The rule-based cues in our task were visual, not auditory, and thus were processed separately from the incoming auditory stream and then incorporated into the auditory decision. Several of our findings imply that this process involved cognitively driven, top-down mechanisms and not lower-level interactions between the visual and auditory stimuli. Specifically, we modeled the rule-based decision biases in terms of computational components of a normative, DDM-based decision process. These kinds of computationally defined biases, which have been studied extensively for visual decision-making (Dunovan et al., 2014; Hanks et al., 2011; Kelly et al., 2020; Mulder et al., 2012; Ratcliff & McKoon, 2008; Seriès & Seitz, 2013) but only sparsely for auditory decision-making (de Gee et al., 2020; Gifford et al., 2014), have been ascribed to top-down influences (Summerfield & de Lange, 2014). Our results further support this idea by showing auditory decision biases can occur flexibly from trial-to-trial, depending on the relationship between the cue and the test stimulus. Moreover, these biases involve computational components that are coordinated with each other, which we previously showed is consistent with a cognitive-based (i.e., not purely stimulus-driven) learning process that can allow individual decision-makers to achieve nearly optimal performance (Fan et al., 2018).

Likewise, the rule-based biases that we measured were accompanied by modulations of pupil size that, like for related findings, appear to be cognitively driven (Joshi & Gold, 2020). Specifically, we found transient pupil increases in response to choices that were incongruent with the prior cue on that trial. These pupil modulations were similar to those that have been reported for other tasks involving decision biases (de Gee et al., 2017, 2014, 2020; Krishnamurthy et al., 2017; Urai et al., 2017), violations of learned expectations (Filipowicz et al., 2020), and certain

task-relevant but not task-irrelevant stimulus changes (Zhao et al., 2019), all of which were interpreted in terms of arousal-linked cognitive influences on perception and/or decision processing. Our work complements and extends these findings by showing that the rule-based effects on task behavior and pupil size can be adjusted from trial-to-trial, based on the current version of the cue and its relationship (congruence) with the test stimulus, further supporting the idea that they are driven by the kinds of flexible information processing associated with top-down control.

Together, these results are consistent with the idea that arousal-linked processes actively monitor and adjust decision-making using relevant predictive cues. These adjustments likely arise from multiple neuromodulatory systems, principally the locus-coeruleus (LC) norepinephrine system and basal forebrain cholinergic system (Joshi & Gold, 2020; Joshi, Li, Kalwani, & Gold, 2016; Reimer et al., 2016), that can affect either bottom-up or top-down information processing in the brain under different conditions. For example, relatively slow fluctuations in baseline or "tonic" arousal levels have been linked to modulation of sensory neurons (Heller, Schwartz, Saderi, & David, 2020; Lin, Asinof, Edwards, & Isaacson, 2019; McGinley, David, & McCormick, 2015; McGinley, Vinck, et al., 2015; Reimer et al., 2014; Schwartz, Buran, & David, 2020; Vinck, Batista-Brito, Knoblich, & Cardin, 2015) and changes in perceptual sensitivity in animal models and human subjects (Gelbard-Sagiv, Magidov, Sharon, Hendler, & Nir, 2018; McGinley, David, et al., 2015; Waschke, Tune, & Obleser, 2019), suggesting bottom-up effects. In contrast, relatively fast, event-driven "phasic" changes in arousal have shown inconsistent relationships to perceptual sensitivity in human subjects (de Gee et al., 2017, 2020). Rather, these phasic changes (like what we measured) are more strongly associated with behaviorally relevant decision- and response-related processes in both humans and animal models (Aston-Jones & Cohen, 2005; de

Gee et al., 2014; Einhäuser, Koch, & Carter, 2010; Kalwani, Joshi, & Gold, 2014), particularly those requiring cognitive or behavioral shifts (Bouret & Sara, 2005), which is suggestive of top-down effects. Our results support this interpretation: the pupil response was modulated by the congruency between the cue and the subject's choice, not the cue and the tone identity, consistent with arousal-linked adjustment of top-down decision biases rather than bottom-up sensory processing. This interpretation accords with a previous visual decision-making study showing that pupil-linked arousal modulates decision biases in frontoparietal regions encoding choice, without any effect on visual cortex (de Gee et al., 2017). Further work is needed to identify whether similar neural dissociations exist in auditory decision-making.

In contrast, the stimulus-based cues appeared to engage a different set of mechanisms that were more consistent with contributions from bottom-up processing. In particular, the stimulus-based cues elicited behavioral biases that included both "attractive" effects (i.e., biases towards previous stimuli) and "repulsive" effects (i.e., biases away from previous stimuli). Indeed, both of these effects have been identified in previous studies of auditory perception (Alais et al., 2015; Chambers et al., 2017; Chambers & Pressnitzer, 2014; Dahmen, Keating, Nodal, Schulz, & King, 2010; Giangrand, Tuller, & Kelso, 2003; Holt & Lotto, 2008; Shu et al., 1993; Snyder, Carter, Hannon, & Alain, 2009) and auditory short-term memory (Lieder et al., 2019). However, most of these prior studies reported consistently attractive or repulsive effects (cf. Snyder et al., 2009 for opposing effects of prior stimuli and prior perception) but not both, leaving us without a principled explanation for the conditions under which one or the other effect should occur. To our knowledge, we are the first to report that the direction of bias depended strongly on SNR, with attractive decision biases predominating for low-test-tone-SNR stimuli and repulsive, adaptation-like mechanisms that reduced sensitivity to repeated stimuli predominating for high-

test-tone-SNR stimuli. The stimulus-based biases were unrelated to rule-based biases and did not show any learning-related coordination within subjects. Moreover, these stimulus-based effects had little relationship to pupil size, unlike the rule-based effects. Thus, these effects did not appear to engage the top-down, arousal-linked cognitive mechanisms used to generate rule-based biases but instead were induced by the tone sequence itself.

These stimulus-based effects were likely driven, in part, by mechanisms of sensory adaptation. These mechanisms affect neural responses throughout the auditory system and generally involve reduced responses to repeated presentation of the same stimuli and potentiated responses to novel (deviant) stimuli (Carbajal & Malmierca, 2018; Näätänen et al., 2007; Nelken, 2014; Sussman, 2007). There is debate over whether these phenomena reflect predictions or whether they are indicative of traditionally construed bottom-up stimulus-specific adaptation, with evidence suggesting that both processes may contribute (Carbajal & Malmierca, 2018; Heilbron & Chait, 2018; Lesicko et al., 2021; Nelken, 2014; Parras et al., 2017; Symonds et al., 2017; Todorovic & de Lange, 2012; Todorovic et al., 2011). Both interpretations are consistent with our findings, in that the attractive effects could reflect predictions whereas the repulsive effects are more consistent with adaptation.

A possible reason for the coexistence of the opposing stimulus-based effects is to allow the brain to navigate the tradeoff between stable integration and change detection as a function of the quality of sensory evidence (Glaze, Kable, & Gold, 2015; Schwiedrzik et al., 2014). When SNR is low, the evidence is unreliable and thus prior expectations are most useful. In contrast, when SNR is high and prior expectations are not as useful, other aspects of stimulus processing can be prioritized, such as increasing sensitivity to deviations from stimulus regularities. Past normative models of evidence accumulation in changing environments have accounted for human subjects'

sensitivity to change via a volatility-dependent leak on the prior accumulated evidence (Glaze et al., 2015). Future work should investigate whether adaptation-induced changes in the encoding of sensory evidence could also account for subject behavior (Fritsche, Spaak, & de Lange, 2020; Schwiedrzik et al., 2014; Stocker & Simoncelli, 2005; Wei & Stocker, 2015), and whether environmental volatility might alter the balance between attractive and repulsive effects in auditory decision making.

In sum, the results of this study established new methods for understanding how stimulus- and rule-based information shape auditory decisions, jointly within a DDM framework. Future work should leverage this framework to identify the neural substrates of these effects and should further establish the stimulus dimensions that govern the balance between attractive and repulsive effects, which has implications for understanding how the brain balances reliance on prior information with sensitivity to change.

Materials and methods

Fifty human subjects participated in the study (19 male, 25 female, 6 N/A; median age: 25 yrs, range 18–60). Informed consent was obtained in accordance with the University of Pennsylvania IRB.

Behavioral Task

Each subject was seated and faced an LCD computer screen (iMac), which sat on a table in a darkened room. The subject listened to auditory stimuli via earphones (Etymotic MC5), while a chin rest stabilized their head for eye tracking. The subject reported whether a "test" tone burst (250 or 2000 Hz; 300-ms duration; 10-ms $\cos^2$ ramp) was "low frequency" or "high frequency" by pressing a button on a gamepad with their left or right index finger, respectively. The test tone was embedded in a background of broadband noise (50–20000 Hz), and we titrated task difficulty by varying the sound level of the test tone (low frequency: 53, 57, 62, and 69 dB SPL; high frequency: 52, 57, 62, and 69 dB SPL) relative to the noise (75 dB SPL). We mapped these signal-to-noise ratios (SNRs) onto a scale from 0.05–0.5, based on the fractional voltage required to generate the test tone at that SNR. Auditory stimuli were generated in the Matlab (R2016a) programming environment.

Most subjects completed 4–5 sessions of the task. Each session began with a set of 60–120 training trials. We then tested a different set of expectation-generating cues per session: "rule-based" cues, "stimulus-based" cues, or both (mixed condition; see Figure 1a). In a rule-based-cue session (576 trials), we presented a visual cue at the beginning of each trial: a triangle pointing to the left indicated 5:1 odds of a low-frequency test tone, a triangle pointing to the right indicated 5:1 odds of a high-frequency test tone, and a square indicated even (neutral) odds. The same cue was presented for a block of 48 trials and was varied randomly between blocks.

In a stimulus-based-cue session (480 trials), we presented a tone-burst sequence (250 or 2000 Hz; 300-ms duration; 10-ms $\cos^2$ ramp; 100-ms inter-burst interval) that preceded the test tone (i.e., the "pre-test" sequence). The pre-test sequence was always presented at the highest SNR. The length of the pre-test sequence varied between 2–14 tones, approximately exponentially distributed. These sequences were pseudorandomly generated, but we ensured that there were approximately the same number of high- and low-frequency tone bursts in each session.

There were also "mixed" sessions in which subjects had both rule-based and stimulus-based cues. In mixed-condition 1, which was divided into two sessions, we used the same rule-based cue (high or low prior) for the entire session (480/trials session) and varied the length of the pre-test sequence. In mixed-condition 2 (576 trials), we randomly varied the rule-based cue and fixed the length of the pre-test sequence at five tone bursts.

Sessions were completed in the following order: rule-based, stimulus-based, mixed-condition 1 (using either a low- or high-prior cue, randomly selected), mixed-condition 1 (using the alternative prior cue), and mixed-condition 2. Because of attrition and other factors, not all subjects completed all conditions: rule-based, N=49 subjects completed the condition; stimulus-based, N=45; mixed-condition 1, N=41, mixed-condition 2, N=21. Further, for all subjects in the stimulus-based session and each session of mixed-condition 1, we discarded 38 trials that did not have a pre-test sequence (which were likely surprising and led to poor subject performance), leaving 442 trials for analysis. Also, one subject completed only 432 trials in the rule-based condition, and two subjects completed only 432 trials in mixed-condition 2. Subjects were paid \$8 plus a performance bonus per session. The bonus was \$1 for each 4% above 50% (max bonus = \$12).

Figure 1b shows the timing of each trial. Subjects could make their response from the start of a visual "go cue", which coincided with the initiation of the test tone, until the trial ended. Subjects were given a 2-s response window, except for 25 subjects in the rule-based condition who were given a 3-s response window. In mixed-condition 2, we did not provide a go cue because the tone-burst sequence had a fixed, predictable duration and thus served as the go cue. Visual and auditory feedback was provided after each trial indicating whether the subject's response was correct or incorrect.

Data analysis

We conducted statistical analyses in R (R Core Team, 2020) and Matlab. Linear mixed-effects models were fit using lme4 (Bates, Mächler, Bolker, & Walker, 2015). When possible, we fit the maximal model (i.e., random intercepts for subjects and random slopes for all within-subjects variables). If the maximal model failed to converge or produced singular fits, we iteratively reduced the random-effects structure until convergence (Bates, Kliegl, Vasishth, & Baayen, 2015). Post-hoc comparisons were conducted using the emmeans package (Lenth, 2016). Post-hoc multiple comparisons were corrected using the Bonferroni-Holm method (Holm, 1979).

We fit a logistic model to the rule-based and stimulus-based psychometric functions using a maximum-likelihood approach. The logistic was of the form:

$$P(H) = \lambda + \frac{1 - 2\lambda}{1 + e^{-f(x)}},$$

where $P(H)$ is the probability that the subject chose high frequency, *f(x)* is a linear function predicting choice, and λ is a lapse rate that sets the lower and upper asymptotes of the logistic curve.

For the rule-based condition, choice was predicted as:

$$f(x) = \beta_0^c + \beta_{SNR} SNR,$$

where β_{SNR} determines the slope of the psychometric function, SNR is the signed signal-to-noise ratio of the test tone (positive: high tones; negative: low tones), and β_0^c determines the bias (offset). To capture the effects of the rule-based cues, we fit separate β_0^c for each prior cue, c (Low, Neutral, High). We also tested a model in which the slope was free to vary with prior cue.

For the stimulus-based condition, choice was predicted as:

$$f(x) = \beta_0 + \beta_{SNR} SNR + \sum_{i=1}^{6} \beta_{pt_i} pt_i + \sum_{i=1}^{6} \beta_{pta_i} pt_i |SNR|,$$

where pt_i is a pre-test tone burst at position i numbered in reverse chronological order (i.e., pt_1 is the tone burst immediately prior to the test tone), β_{pt_i} determines the bias (offset) attributable to each tone burst, and β_0 is a fixed offset capturing any idiosyncratic biases. The pt_i were contrast coded such that β_{pt_i} is the log-odds ratio of choosing high frequency over low frequency at a SNR of 0 (high-frequency regression contrast code: 0.5; low-frequency regression contrast code: −0.5). We modeled a SNR-dependent adaptation-like effect as the interaction term $pt_i|SNR|$: $|SNR|$ is the unsigned signal-to-noise ratio of the test tone, and each β_{pta_i} determines how much each tone burst influences the slope of the psychometric function. We fit data only for the last six pre-test tone bursts because longer tone-burst sequences were infrequent.

Model Comparison

We assessed goodness-of-fit using Akaike information criteria (AIC). We also entered the AIC values into a Bayesian random-effects analysis, which attempts to identify the model among competing alternatives that is most prevalent in the population. This analysis yields a protected

exceedance probability (PEP) for each model, which is the probability that the model is the most frequent in the population, above and beyond chance (Rigoux, Stephan, Friston, & Daunizeau, 2014). PEPs were computed using the VBA toolbox (Daunizeau, Adam, & Rigoux, 2014).

Drift-diffusion modeling (DDM)

We used PyDDM (Shinn et al., 2020) for all DDM analyses except for the simulations of the different types of biases, which were generated using an analytical solution to the DDM (Palmer et al., 2005). Unlike some of the fits described below, these simulations have a fixed bound and were not fit to the data but rather used ranges of parameter values that generated psychometric and chronometric functions that were qualitatively consistent with the data.

In the DDM framework, noisy evidence is accumulated until reaching one of the two bounds, triggering commitment to one of the two choices (in this case, low frequency or high frequency). In our implementation, bound height was determined by a parameter B, which was equal to half the total distance between the bounds. All models, except as noted, included a linear collapsing bound, which accounts for the truncated RT distributions given that subjects were under time pressure. (RT was the time between onset of the go cue and gamepad button press, except for mixed-condition 2 in which a subject's RT was the time between test-tone offset and button press.) Thus, B was the initial bound height, and an additional parameter t_B determined the rate of linear collapse, such that total bound height at time t was $2(B - t_B t)$.

The full slope or rate of evidence accumulation was defined as:

$$slope = v_{SNR} SNR + bias_{evidence} + adapt * |SNR|,$$

where v_{SNR} is the drift rate, which influences the rate at which the sensory evidence provided by the test tone in the noisy background, *SNR,* contributes to evidence accumulation.

We defined separate $bias_{evidence}$ terms for different expectation-generating cue conditions. For the rule-based condition, $bias_{evidence}$ was set to one of three parameters depending on the prior cue (low: v_{Low}; $neutral$: v_0; $high$: v_{High}). For the stimulus-based condition, $bias_{evidence} = v_0 + v_{Bias} pt_{Bias}$, where v_0 is a fixed offset capturing any idiosyncratic bias toward high or low and pt_{Bias} is an exponentially weighted sum of the pre-test tone bursts:

$$pt_{Bias} = \sum_{i \in high} e^{-\frac{pt_i}{\tau_{Bias}}} - \sum_{j \in low} e^{-\frac{pt_j}{\tau_{Bias}}},$$

where pt_i and pt_j are the sequence positions (numbered in reverse chronological order starting at 0) of the high- and low-frequency tone bursts in the pre-test sequence, respectively; τ_{Bias} is a time constant determining the decay in influence of the tone bursts with increasing temporal distance from the test tone; and v_{Bias} scales the total influence of the tone bursts on the rate of evidence accumulation.

The full stimulus-based model also included an adaptation-like term in the slope, $adapt * |SNR|$. The *adapt* quantity was defined as

$$adapt = va_{High} \sum_{i \in high} e^{-\frac{pt_i}{\tau_{va}}} - va_{Low} \sum_{j \in low} e^{-\frac{pt_j}{\tau_{va}}},$$

where τ_{va} is a time constant and va_{High} and va_{Low} are separate weights for the high- and low-frequency tone bursts.

Our model also controlled the location between the two bounds at which evidence starts accumulating. If the starting point is not equidistant between the two bounds, less evidence is required to make one choice versus the other; i.e., a starting-point bias. The starting point was defined as

$$starting\ point = bias_{start} * 2B,$$

where $2B$ is the total bound height, and $bias_{start}$ is the bias on the starting point, expressed as a fraction of total bound height [0,1] (i.e., a value of 0.5 corresponds to an unbiased starting point, equidistant between the bounds). For the rule-based condition, $bias_{start}$was set to one of three parameters depending on which prior cue was presented on that trial (low: z_{Low}; $neutral$: z_0; $high$: z_{High}). For the stimulus-based condition, $bias_{start} = g(z_0 + z_{Bias}pt_{Bias})$. The pt_{Bias} was the same quantity as in the evidence-accumulation term, z_{Bias} scaled the total influence of the tone bursts in the pre-test sequence on the starting point, and z_0 was a fixed offset accounting for idiosyncratic starting-point biases. The function *g(x)* was the logistic function, $\frac{1}{1+e^{-x}}$, which constrained $bias_{start}$ between 0 and 1. We did not fit the rule-based condition using this logistic transformation; however, we transformed the resulting parameter estimates to the logit scale to be more comparable with the stimulus-based fits.

In addition to these parameters, all models were fit with a non-decision time, ndt_0, which accounted for the portion of RT not determined by decision formation (e.g., sensory or motor processing). For the stimulus-based condition, RTs were faster when the pre-test tone bursts were the same frequency. To account for this effect, total non-decision time was calculated as

$$ndt = ndt_0 + ndt_{Bias}|pt_{Bias}|,$$

where the extra additive term is the absolute value of the stimulus-based bias calculated above, weighted by ndt_{Bias}.

Finally, all models were fit with a lapse rate, λ, which mixed the RT distribution predicted by the DDM with a uniform distribution in proportion to λ (i.e., $\lambda = 0.05$ implies that the final

predicted distribution was a weighted average of 95% the DDM distribution and 5% a uniform distribution).

We fit models separately to each task condition. See Shinn et al. (2020) for details of the optimization procedure. Models for the mixed conditions were identical to those described above but included both types of bias. For the rule- and stimulus-based conditions, we also fit reduced models to assess the necessity of different mechanisms for explaining subjects' behavior. The "base" model was a standard DDM augmented by idiosyncratic bias terms for evidence accumulation and starting point but without rule- or stimulus-based biases; it included six parameters, $v_{SNR}, B, v_0, z_0, ndt_0, \lambda$. The "collapsing bound" model included one additional parameter, t_B. The "full" model in the rule-based condition and the "stimulus-based bias" model in the stimulus-based condition included the $bias_{evidence}$ and $bias_{start}$ (and $ndt_{bias}$for the stimulus-based condition) terms, for a total of 11 parameters each. The "full" model in the stimulus-based condition further included the $adapt$ term, for a total of 14 parameters.

We used the full-model fits to generate performance functions for each subject. The output of the performance function, $pc(z, v|c, \theta)$, was the predicted percentage of correct choices for a given combination of starting-point bias (z) and evidence-accumulation bias (v), given the expectation-cue context (c) and the subject's other best-fitting DDM parameters (θ). For the rule-based condition, the performance function was estimated for the context of the low prior and the high prior. For the stimulus-based condition, the context was set to either two low-frequency pre-test tone bursts (LL) or two high-frequency pre-test tone bursts (HH). These tone bursts did not change the odds that the test tone would be low or high but nonetheless affected performance, as quantified via bias and adaptation-like effects in the DDM fits.

We estimated the performance function across a grid of z, v values (z: $(.1, .9)$; v: $[-4,4]$), where z dictated the value of z_{Low} or z_{High} in the rule-based condition and z_{Bias} in the stimulus-based condition, and v dictated the value of v_{Low} or v_{High} in the rule-based condition and v_{Bias} in the stimulus-based condition. The predicted percent correct was generated from the DDM for each point on the grid for all combinations of test-tone frequency value and SNR. Next, these values were averaged according to the proportion of each trial type expected in that context. This procedure was implemented separately for each subject, condition, and context. The resulting performance functions were then normalized to a proportion of maximum possible performance scale by dividing by the maximum accuracy obtained for each function. Performance functions were then averaged across subjects for each context, and subject-averaged 97% contours were plotted using the Matlab contour function.

We fit a mixed-effects model to test whether the slope of the relationship between the starting-point and evidence-accumulation biases differed between the rule- and stimulus-based conditions. We entered the starting-point bias as the predictor and assessed the interaction between starting-point bias and bias type (z_{High}, z_{Low}, or z_{Bias}) in predicting the evidence-accumulation bias. Specifically, we contrasted the slopes of the rule-based and stimulus-based biases ([average of z_{High} and z_{Low}] $-$ z_{Bias}) and the contrast of the rule-based slopes ($z_{High} - z_{Low}$). To confirm that the results were not dependent on which variable was entered as the outcome and which as the predictor, we re-estimated the model with the evidence-accumulation bias as predictor and starting point bias as outcome, which yielded similar results (rule-based vs. stimulus-based: $B = 0.47$, $t(53.65) = 2.93$, $p = 0.005$; rule-based high vs. low ($B = -0.21$, $t(118.93) = -0.93$, $p > 0.05$). Because the rule- and stimulus-based biases are on different scales, for both models, the bias variables were z-scored within condition.

To test the association between rule-based and stimulus-based bias parameters, we calculated the rule-based biases for a given condition as the difference between the high and low bias for both evidence-accumulation (i.e., $v_{High} - v_{Low}$) and starting-point (i.e., $z_{High} - z_{Low}$) biases. We then calculated the Spearman's correlation between these quantities and v_{Bias} and z_{Bias}, respectively.

Pupillometry

We recorded (EyeLink 1000 Plus; SR Research) each subject's right-eye position and pupil diameter at a sampling rate of 1000 Hz. Each subject maintained their gaze within a 14.66 x 8.11° window throughout the trial.

If data were missing, either due to blinks or other artifacts, we linearly interpolated the pupil data after removing ±100 ms surrounding the blink (or artifact). We identified additional artifacts by computing the difference between consecutive samples of the pupil time course and removed all high-velocity periods (i.e., > 24 a.u./ms). If the duration of any of these periods exceeded 16 ms, we also removed the ±100 ms of surrounding data. These artifactual periods were then filled via linear interpolation. We also interpolated gaze-position data for time points missing or removed from the pupil time course. We excluded trials in which >50% of the pupil data and sessions in which >60% of the pupil data were missing or were artifactual from further pupil analysis. Additionally, in mixed-condition 1, both sessions had to pass these criteria for the subject to be included in the pupil analysis.

The pupil time course was then low-pass filtered with an 8-Hz cutoff. We z-scored each subject's time course within each block. For every trial, we calculated the baseline pupil diameter as the

average diameter from 0–40 ms relative to test-tone onset, which was then subtracted from the trial time course.

Gaze position for each trial was centered on the average gaze position during the baseline period. For each session, we defined the fixation window as a circle containing 95% of gaze samples across all data (1.36–3.29° visual angle across sessions). To minimize the impact of eye movements on pupil diameter, we excluded trials in which gaze deviated from this window for >15 ms.

Finally, we excluded subjects with fewer than 75 trials remaining in a condition after all cleaning procedures. Overall, we analyzed 44 subjects in the rule-based condition, 42 in the stimulus-based condition, 33 in mixed-condition 1, and 17 in mixed-condition 2.

For statistical analyses, we downsampled the eye data to 50 Hz. Like for the RT analyses, we analyzed pupil diameter with respect to the congruence between the cue and choice and restricted our main analyses to correct trials to avoid confounding changes in pupil size with feedback/error related signals or off-task responses. We analyzed the rule- and stimulus-based conditions by fitting a linear mixed-effects model to the data at every time point. These analyses focused on contrasts of the pupil time course as a function of the congruency of choice with the rule- and stimulus-based cues (e.g., incongruent – congruent), and the interaction of congruency with |SNR|. All models controlled for test-tone frequency, |SNR|, baseline pupil diameter, and gaze position. Data were aligned to choice (i.e., the time of the button press).

To test the association between behavioral bias and the congruency effects in the rule-based condition, separate linear models were fit to the pupil data per subject to obtain estimates of individual-subject congruency contrasts. These contrasts were then correlated across time with

the estimate of behavioral bias obtained from the logistic fits to the psychometric function described above, where bias was defined as $\beta_0^{High} - \beta_0^{Low}$. We used FDR correction to adjust *p*-values for multiple comparison across time (Benjamini & Hochberg, 1995; Yekutieli & Benjamini, 1999). Congruency contrasts were corrected together across time and contrast.

Acknowledgements

YEC, JIG, and LSA received support for this work from an Office of Naval Research grant [N000141612539]. NT was supported by a T32 training grant from the National Institutes of Health [MH014654].

Competing interests

JIG: Senior editor, *eLife.* The authors declare that they have no other competing interests.

Data availability

The datasets generated and analyzed for this article will be made available prior to publication at: https://osf.io/f9nyr/. The analysis code for this article will be made available prior to publication at: https://github.com/TheGoldLab/Analysis_Tardiff_etal_AuditoryPriors.

References

Alais, D., Orchard-Mills, E., & Van der Burg, E. (2015). Auditory frequency perception adapts rapidly to the immediate past. *Attention, Perception, and Psychophysics*, *77*(3), 896–906. https://doi.org/10.3758/s13414-014-0812-2

Aston-Jones, G., & Cohen, J. D. (2005). An integrative theory of locus coeruleus-norepinephrine function: adaptive gain and optimal performance. *Annual Review of Neuroscience*, *28*(1), 403–450. https://doi.org/10.1146/annurev.neuro.28.061604.135709

Bastos, A. M., Lundqvist, M., Waite, A. S., Kopell, N., & Miller, E. K. (2020). Layer and rhythm specificity for predictive routing. *Proceedings of the National Academy of Sciences of the United States of America*, *117*(49), 31459–31469. https://doi.org/10.1073/pnas.2014868117

Bastos, A. M., Usrey, W. M., Adams, R. A., Mangun, G. R., Fries, P., & Friston, K. J. (2012). Canonical Microcircuits for Predictive Coding. *Neuron*, *76*(4), 695–711. https://doi.org/10.1016/j.neuron.2012.10.038

Bates, D., Kliegl, R., Vasishth, S., & Baayen, H. (2015). Parsimonious Mixed Models. https://doi.org/arXiv:1506.04967

Bates, D., Mächler, M., Bolker, B., & Walker, S. (2015). Fitting linear mixed-effects models using lme4. *Journal of Statistical Software*, *67*(1), 1–48. https://doi.org/10.18637/jss.v067.i01

Benjamini, Y., & Hochberg, Y. (1995). Controlling the False Discovery Rate: A Practical and Powerful Approach to Multiple Testing. *Journal of the Royal Statistical Society: Series B (Methodological)*, *57*(1), 289–300. https://doi.org/10.1111/j.2517-6161.1995.tb02031.x

Bouret, S., & Sara, S. J. (2005). Network reset: A simplified overarching theory of locus coeruleus noradrenaline function. *Trends in Neurosciences*, *28*(11), 574–582. https://doi.org/10.1016/j.tins.2005.09.002

Carbajal, G. V., & Malmierca, M. S. (2018). The Neuronal Basis of Predictive Coding Along the Auditory Pathway: From the Subcortical Roots to Cortical Deviance Detection. *Trends in Hearing*, *22*, 1–33. https://doi.org/10.1177/2331216518784822

Chambers, C., Akram, S., Adam, V., Pelofi, C., Sahani, M., Shamma, S., & Pressnitzer, D. (2017). Prior context in audition informs binding and shapes simple features. *Nature Communications*, *8*. https://doi.org/10.1038/ncomms15027

Chambers, C., & Pressnitzer, D. (2014). Perceptual hysteresis in the judgment of auditory pitch shift. *Attention, Perception, and Psychophysics*, *76*(5), 1271–1279. https://doi.org/10.3758/s13414-014-0676-5

Dahmen, J. C., Keating, P., Nodal, F. R., Schulz, A. L., & King, A. J. (2010). Adaptation to Stimulus Statistics in the Perception and Neural Representation of Auditory Space. *Neuron*, *66*(6), 937–948. https://doi.org/10.1016/j.neuron.2010.05.018

Daunizeau, J., Adam, V., & Rigoux, L. (2014). VBA: A probabilistic treatment of nonlinear models for neurobiological and behavioural data. *PLoS Computational Biology*, *10*(1),

e1003441. https://doi.org/10.1371/journal.pcbi.1003441

de Gee, J. W., Colizoli, O., Kloosterman, N. A., Knapen, T., Nieuwenhuis, S., Donner, T. H., … Matthews, P. (2017). Dynamic modulation of decision biases by brainstem arousal systems. *ELife*, *6*, 1127–1141. https://doi.org/10.7554/eLife.23232

de Gee, J. W., Knapen, T., & Donner, T. H. (2014). Decision-related pupil dilation reflects upcoming choice and individual bias. *Proceedings of the National Academy of Sciences of the United States of America*, *111*(5), E618-25. https://doi.org/10.1073/pnas.1317557111

de Gee, J. W., Tsetsos, K., Schwabe, L., Urai, A. E., McCormick, D., McGinley, M. J., & Donner, T. H. (2020). Pupil-linked phasic arousal predicts a reduction of choice bias across species and decision domains. *ELife*, *9*. https://doi.org/10.7554/eLife.54014

de Lange, F. P., Heilbron, M., & Kok, P. (2018). How Do Expectations Shape Perception? *Trends in Cognitive Sciences*, *22*(9), 764–779. https://doi.org/10.1016/J.TICS.2018.06.002

Doi, T., Fan, Y., Gold, J. I., & Ding, L. (2020). The caudate nucleus contributes causally to decisions that balance reward and uncertain visual information. *ELife*, *9*, 568733. https://doi.org/10.7554/eLife.56694

Dunovan, K. E., Tremel, J. J., & Wheeler, M. E. (2014). Prior probability and feature predictability interactively bias perceptual decisions. *Neuropsychologia*, *61*(1), 210–221. https://doi.org/10.1016/J.NEUROPSYCHOLOGIA.2014.06.024

Einhäuser, W., Koch, C., & Carter, O. L. (2010). Pupil dilation betrays the timing of decisions. *Frontiers in Human Neuroscience*, *4*, 18. https://doi.org/10.3389/fnhum.2010.00018

Fan, Y., Gold, J. I., & Ding, L. (2018). Ongoing, rational calibration of reward-driven perceptual biases. *ELife*, *7*. https://doi.org/10.7554/eLife.36018

Filipowicz, A. L. S., Glaze, C. M., Kable, J. W., & Gold, J. I. (2020). Pupil diameter encodes the idiosyncratic, cognitive complexity of belief updating. *ELife*, *9*. https://doi.org/10.7554/eLife.57872

Fischer, J., & Whitney, D. (2014). Serial dependence in visual perception. *Nature Neuroscience 2014 17:5*, *17*(5), 738–743. https://doi.org/10.1038/nn.3689

Fritsche, M., Spaak, E., & de Lange, F. P. (2020). A Bayesian and efficient observer model explains concurrent attractive and repulsive history biases in visual perception. *ELife*, *9*. https://doi.org/10.7554/eLife.55389

Gelbard-Sagiv, H., Magidov, E., Sharon, H., Hendler, T., & Nir, Y. (2018). Noradrenaline Modulates Visual Perception and Late Visually Evoked Activity. *Current Biology*, *28*(14), 2239-2249.e6. https://doi.org/10.1016/j.cub.2018.05.051

Giangrand, J., Tuller, B., & Kelso, J. A. S. (2003). Perceptual Dynamics of Circular Pitch. *Music Perception*, *20*(3), 241–262. https://doi.org/10.1525/mp.2003.20.3.241

Gifford, A. M., Cohen, Y. E., & Stocker, A. A. (2014). Characterizing the Impact of Category Uncertainty on Human Auditory Categorization Behavior. *PLoS Computational Biology*, *10*(7). https://doi.org/10.1371/journal.pcbi.1003715

Glaze, C. M., Kable, J. W., & Gold, J. I. (2015). Normative evidence accumulation in unpredictable environments. *ELife*, *4*(AUGUST2015). https://doi.org/10.7554/eLife.08825

Hanks, T. D., Mazurek, M. E., Kiani, R., Hopp, E., & Shadlen, M. N. (2011). Elapsed decision time affects the weighting of prior probability in a perceptual decision task. *Journal of Neuroscience*, *31*(17), 6339–6352. https://doi.org/10.1523/JNEUROSCI.5613-10.2011

Heilbron, M., & Chait, M. (2018). Great Expectations: Is there Evidence for Predictive Coding in Auditory Cortex? *Neuroscience*, *389*, 54–73. https://doi.org/10.1016/J.NEUROSCIENCE.2017.07.061

Heller, C. R., Schwartz, Z. P., Saderi, D., & David, S. V. (2020, September 1). Selective effects of arousal on population coding of natural sounds in primary auditory cortex. *BioRxiv*. bioRxiv. https://doi.org/10.1101/2020.08.31.276584

Holm, S. (1979). A simple sequentially rejective multiple test procedure. *Scandinavian Journal of Statistics*, *6*, 65–70. https://doi.org/10.2307/4615733

Holt, L. L., & Lotto, A. J. (2008). Speech perception within an auditory cognitive science framework. *Current Directions in Psychological Science*, *17*(1), 42–46. https://doi.org/10.1111/j.1467-8721.2008.00545.x

Joshi, S., & Gold, J. I. (2020). Pupil size as a window on neural substrates of cognition. *Trends in Cognitive Sciences*, *24*(6), 466–480. https://doi.org/10.1016/j.tics.2020.03.005

Joshi, S., Li, Y., Kalwani, R. M., & Gold, J. I. (2016). Relationships between pupil diameter and neuronal activity in the locus coeruleus, colliculi, and cingulate cortex. *Neuron*, *89*(1), 221–234. https://doi.org/10.1016/j.neuron.2015.11.028

Kalwani, R. M., Joshi, S., & Gold, J. I. (2014). Phasic Activation of Individual Neurons in the Locus Ceruleus/Subceruleus Complex of Monkeys Reflects Rewarded Decisions to Go But Not Stop. *The Journal of Neuroscience*, *34*(41), 13656–13669. https://doi.org/10.1523/JNEUROSCI.2566-14.2014

Kelly, S. P., Corbett, E. A., & O'Connell, R. G. (2020). Neurocomputational mechanisms of prior-informed perceptual decision-making in humans. *Nature Human Behaviour*, *5*(4), 467–481. https://doi.org/10.1038/s41562-020-00967-9

Krishnamurthy, K., Nassar, M. R., Sarode, S., & Gold, J. I. (2017). Arousal-related adjustments of perceptual biases optimize perception in dynamic environments. *Nature Human Behaviour*, *1*(6), 0107. https://doi.org/10.1038/s41562-017-0107

Lenth, R. V. (2016). Least-squares means: The R package lsmeans. *Journal of Statistical Software*, *69*(1), 1–33. https://doi.org/10.18637/jss.v069.i01

Lesicko, A. M. H., Angeloni, C. F., Blackwell, J. M., De Biasi, M., & Geffen, M. N. (2021). Cortico-Fugal Regulation of Predictive Coding. *BioRxiv*, 2021.04.12.439188. https://doi.org/10.1101/2021.04.12.439188

Lieder, I., Adam, V., Frenkel, O., Jaffe-Dax, S., Sahani, M., & Ahissar, M. (2019). Perceptual bias reveals slow-updating in autism and fast-forgetting in dyslexia. *Nature Neuroscience*, *22*(2), 256–264. https://doi.org/10.1038/s41593-018-0308-9

Lin, P.-A., Asinof, S. K., Edwards, N. J., & Isaacson, J. S. (2019). Arousal regulates frequency tuning in primary auditory cortex. *Proceedings of the National Academy of Sciences*, 201911383. https://doi.org/10.1073/pnas.1911383116

McGinley, M. J., David, S. V., & McCormick, D. A. (2015). Cortical Membrane Potential Signature of Optimal States for Sensory Signal Detection. *Neuron*, *87*(1), 179–192. https://doi.org/10.1016/j.neuron.2015.05.038

McGinley, M. J., Vinck, M., Reimer, J., Batista-Brito, R., Zagha, E., Cadwell, C. R., … McCormick, D. A. (2015). Waking state: Rapid variations modulate neural and behavioral responses. *Neuron*, *87*(6), 1143–1161. https://doi.org/10.1016/j.neuron.2015.09.012

Mulder, M. J., Wagenmakers, E. J., Ratcliff, R., Boekel, W., & Forstmann, B. U. (2012). Bias in the brain: A diffusion model analysis of prior probability and potential payoff. *Journal of Neuroscience*, *32*(7), 2335–2343. https://doi.org/10.1523/JNEUROSCI.4156-11.2012

Näätänen, R., Paavilainen, P., Rinne, T., & Alho, K. (2007). The mismatch negativity (MMN) in basic research of central auditory processing: A review. *Clinical Neurophysiology*, *118*(12), 2544–2590. https://doi.org/10.1016/j.clinph.2007.04.026

Nelken, I. (2014). Stimulus-specific adaptation and deviance detection in the auditory system: experiments and models. *Biological Cybernetics*, *108*(5), 655–663. https://doi.org/10.1007/s00422-014-0585-7

Palmer, J., Huk, A. C., & Shadlen, M. N. (2005). The effect of stimulus strength on the speed and accuracy of a perceptual decision. *Journal of Vision*, *5*(5), 1–1. https://doi.org/10.1167/5.5.1

Parras, G. G., Nieto-Diego, J., Carbajal, G. V., Valdés-Baizabal, C., Escera, C., & Malmierca, M. S. (2017). Neurons along the auditory pathway exhibit a hierarchical organization of prediction error. *Nature Communications*, *8*(1), 1–17. https://doi.org/10.1038/s41467-017-02038-6

Pérez-González, D., Hernández, O., Covey, E., & Malmierca, M. S. (2012). GABA A-mediated inhibition modulates stimulus-specific adaptation in the inferior colliculus. *PLoS ONE*, *7*(3), e34297. https://doi.org/10.1371/journal.pone.0034297

R Core Team. (2020). R: A language and environment for statistical computing. Vienna, Austria: R Foundation for Statistical Computing. Retrieved from https://www.r-project.org

Ratcliff, R., & McKoon, G. (2008). The diffusion decision model: Theory and data for two-choice decision tasks. *Neural Computation*, *20*(4), 873–922. https://doi.org/10.1162/neco.2008.12-06-420

Reimer, J., Froudarakis, E., Cadwell, C. R., Yatsenko, D., Denfield, G. H., & Tolias, A. S. (2014). Pupil fluctuations track fast switching of cortical states during quiet wakefulness. *Neuron*, *84*(2), 355–362. https://doi.org/10.1016/j.neuron.2014.09.033

Reimer, J., McGinley, M. J., Liu, Y., Rodenkirch, C., Wang, Q., McCormick, D. A., & Tolias, A. S. (2016). Pupil fluctuations track rapid changes in adrenergic and cholinergic activity in cortex. *Nature Communications*, *7*(1), 13289. https://doi.org/10.1038/ncomms13289

Rigoux, L., Stephan, K. E., Friston, K. J., & Daunizeau, J. (2014). Bayesian model selection for group studies - Revisited. *NeuroImage*, *84*, 971–985. https://doi.org/10.1016/j.neuroimage.2013.08.065

Schwartz, Z. P., Buran, B. N., & David, S. V. (2020). Pupil-associated states modulate excitability but not stimulus selectivity in primary auditory cortex. *Journal of Neurophysiology*, *123*(1), 191–208. https://doi.org/10.1152/jn.00595.2019

Schwiedrzik, C. M., Ruff, C. C., Lazar, A., Leitner, F. C., Singer, W., & Melloni, L. (2014). Untangling perceptual memory: Hysteresis and adaptation map into separate cortical networks. *Cerebral Cortex*, *24*(5), 1152–1164. https://doi.org/10.1093/cercor/bhs396

Seriès, P., & Seitz, A. R. (2013). Learning what to expect (in visual perception). *Frontiers in Human Neuroscience*, *7*(OCT), 1–14. https://doi.org/10.3389/fnhum.2013.00668

Shinn, M., Lam, N. H., & Murray, J. D. (2020). A flexible framework for simulating and fitting generalized drift-diffusion models. *ELife*, *9*, 1–27. https://doi.org/10.7554/ELIFE.56938

Shu, Z. J., Swindale, N. V., & Cynader, M. S. (1993). Spectral motion produces an auditory after-effect. *Nature*, *364*(6439), 721–723. https://doi.org/10.1038/364721a0

Snyder, J. S., Carter, O. L., Hannon, E. E., & Alain, C. (2009). Adaptation Reveals Multiple Levels of Representation in Auditory Stream Segregation. *Journal of Experimental Psychology: Human Perception and Performance*, *35*(4), 1232–1244. https://doi.org/10.1037/a0012741

Sotiropoulos, G., Seitz, A. R., & Seris, P. (2011). Changing expectations about speed alters perceived motion direction. *Current Biology*, *21*(21), R883–R884. https://doi.org/10.1016/J.CUB.2011.09.013

Stocker, A. A., & Simoncelli, E. P. (2005). Sensory adaptation within a Bayesian framework for perception. In *Advances in Neural Information Processing Systems* (Vol. 18, pp. 1289–1296). MIT Press.

Summerfield, C., & de Lange, F. P. (2014). Expectation in perceptual decision making: neural and computational mechanisms. *Nature Reviews Neuroscience*, *15*(11), 745–756. https://doi.org/10.1038/nrn3838

Sussman, E. S. (2007). A new view on the MMN and attention debate: The role of context in processing auditory events. *Journal of Psychophysiology*, *21*(3–4), 164–175. https://doi.org/10.1027/0269-8803.21.34.164

Symonds, R. M., Lee, W. W., Kohn, A., Schwartz, O., Witkowski, S., & Sussman, E. S. (2017). Distinguishing Neural Adaptation and Predictive Coding Hypotheses in Auditory Change Detection. *Brain Topography*, *30*(1), 136–148. https://doi.org/10.1007/s10548-016-0529-8

Todorovic, A., & de Lange, F. P. (2012). Repetition suppression and expectation suppression are dissociable in time in early auditory evoked fields. *Journal of Neuroscience*, *32*(39), 13389–13395. https://doi.org/10.1523/JNEUROSCI.2227-12.2012

Todorovic, A., van Ede, F., Maris, E., & de Lange, F. P. (2011). Prior expectation mediates neural adaptation to repeated sounds in the auditory cortex: An MEG study. *Journal of*

Neuroscience, *31*(25), 9118–9123. https://doi.org/10.1523/JNEUROSCI.1425-11.2011

Tsunada, J., Cohen, Y., & Gold, J. I. (2019). Post-decision processing in primate prefrontal cortex influences subsequent choices on an auditory decision-making task. *ELife*, *8*. https://doi.org/10.7554/eLife.46770.001

Urai, A. E., Braun, A., & Donner, T. H. (2017). Pupil-linked arousal is driven by decision uncertainty and alters serial choice bias. *Nature Communications*, *8*(1), 14637. https://doi.org/10.1038/ncomms14637

Vinck, M., Batista-Brito, R., Knoblich, U., & Cardin, J. A. (2015). Arousal and Locomotion Make Distinct Contributions to Cortical Activity Patterns and Visual Encoding. *Neuron*, *86*(3), 740–754. https://doi.org/10.1016/j.neuron.2015.03.028

Waschke, L., Tune, S., & Obleser, J. (2019). Local cortical desynchronization and pupil-linked arousal differentially shape brain states for optimal sensory performance. *ELife*, *8*. https://doi.org/10.7554/eLife.51501

Wei, X. X., & Stocker, A. A. (2015). A Bayesian observer model constrained by efficient coding can explain "anti-Bayesian" percepts. *Nature Neuroscience*, *18*(10), 1509–1517. https://doi.org/10.1038/nn.4105

Yekutieli, D., & Benjamini, Y. (1999). Resampling-based false discovery rate controlling multiple test procedures for correlated test statistics. *Journal of Statistical Planning and Inference*, *82*(1–2), 171–196. https://doi.org/10.1016/s0378-3758(99)00041-5

Zhao, S., Chait, M., Dick, F., Dayan, P., Furukawa, S., & Liao, H.-I. I. (2019). Pupil-linked phasic arousal evoked by violation but not emergence of regularity within rapid sound sequences. *Nature Communications*, *10*(1), 4030. https://doi.org/10.1038/s41467-019-12048-1

Supplementary Figures

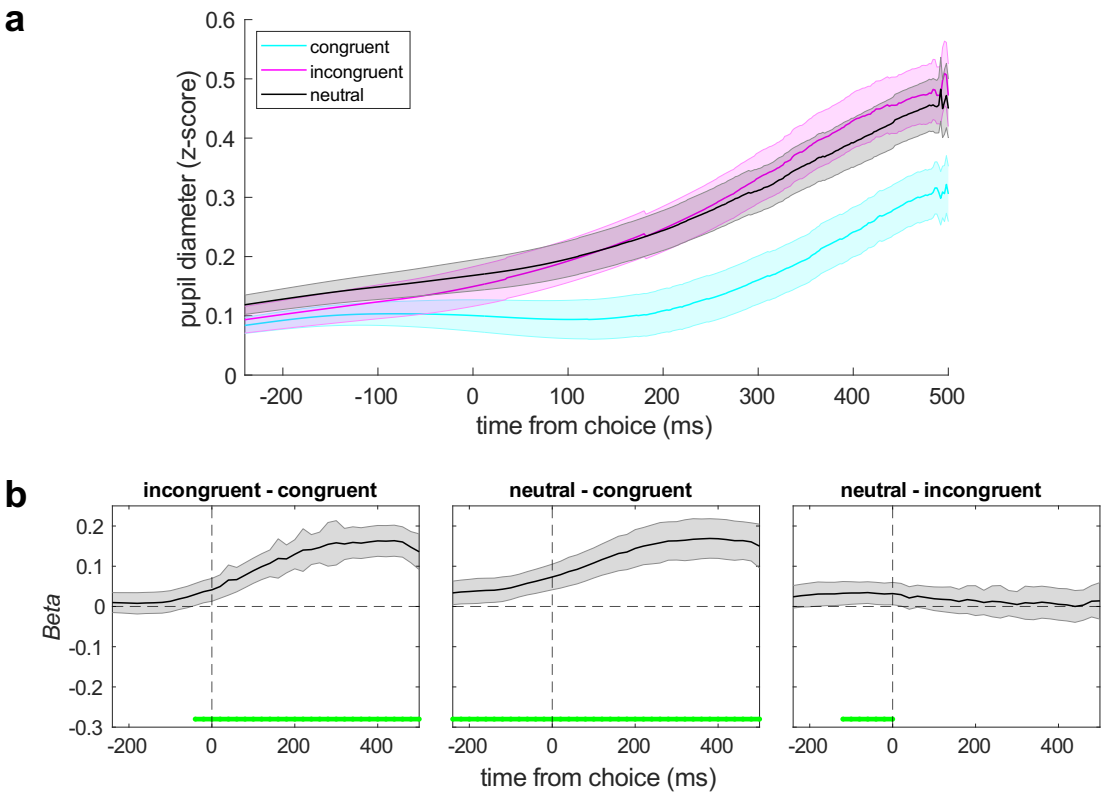

Figure 5–Figure supplement 1. **Rule-based cues modulated pupil-linked arousal on incorrect trials**. **a** Pupil diameter on incorrect trials, aligned to choice and plotted as a function of the congruence between the choice and the prior. Lines and error bars are means and SEM across all trials and subjects. **b** Regression coefficients (beta values) from a linear mixed-effects model as a function of different pupil contrasts (see labels above each panel). Error bars are 95% confidence intervals of the parameter estimates. The time window in **a** and **b** begins earlier than the corresponding window from Figure 5 to focus on the time period in which the incongruent – congruent effect was most prominent in the correct trials. The window ends earlier because incorrect trials were programmed to end faster than correct trials. Values in **b** were computed in 20 ms-wide time bins. Green lines indicate time bins for which $p_{\text{corrected}} < 0.05$, FDR-corrected across time and contrast.